FEDERAL UNIVERSITY OF SANTA CATARINA
JOINVILLE TECHNOLOGY CENTER
UNDERGRADUATE COURSE IN MECHATRONIC ENGINEERING

HENRIQUE MAIOCHI

FEASIBILITY STUDY OF MULTI-STAGE SLURRY-JET MILLING OF CERAMICS

Joinville
2023

HENRIQUE MAIOCHI

FEASIBILITY STUDY OF MULTI-STAGE SLURRY-JET MILLING OF CERAMICS

This graduation thesis is presented to fulfill the partial requirement to obtain the title of bachelor in the course of Mechatronic Engineering, at the Joinville Technology Center, from the Federal University of Santa Catarina.
Supervisor: Prof. Pablo Andretta Jaskowiak, Dr.
Co-supervisor: Manuel Schüler, M.Sc.

Joinville
2023

To all the incredible people that I met during the last year, from who I learned more than what could ever be described into a written-thesis.

A todas as incríveis pessoas que conheci durante o último ano, e que aprendi mais do que poderia ser descrito em uma tese.

ACKNOWLEDGEMENTS

Once again, huge thanks to all the people that were around while I was doing this work. In special to my advisors, supervisors, and friends, that not only supported me but were and continue to be an inspiration to the person I want to be.

Even more, special acknowledgements to my mom, dad, brother and auntie. Always present when I needed, more than as friends, but also as family.

I am also grateful for the unique opportunities I had to learn inside institutions like Fraunhofer Institute IPT, Federal University of Santa Catarina UFSC and the Research Group on Computer Aided Manufacturing GPCAM.

To the friends from UFSC, Joinville and Itajaí, to whom I will certainly show this as soon as I see them again. To the friends I made at GPCAM, and Professor Fagali to be my advisor during the years I spent there. Professor Pablo, for helping more than just as an advisor. To the friends and colleagues I have met thankfully to IPT 300, Fabinho, Vitinho, Tapetito, Laura, Dimmy, Luiza, Gustavo, Koiko. And friends from Aachen from all the random and special moments that we passed together. Thanks also to my supervisor Henrik and the other research assistants that taught me important lessons during my internship there.

At last but not least, huge thanks to my advisor Manuel Schüler for guiding me during the research presented on these pages, always with such unique enthusiasm.

”The worst surroundings in the world
can be tolerated if the people in them
are interesting and kind.”
(Lemony Snicket, 1999)

ABSTRACT

Some conventional manufacturing methods, such as the ones that make use of milling cutters, are not easily applicable when dealing with very hard and brittle materials or when they are thermally sensitive. In those cases, the use of unconventional methods such as Abrasive Water Jet (AWJ) and its variations have some benefits. Milling with Abrasive Water-jets has still several points for improvement. Different approaches are also available for what type of jet is used, such as with Slurry Injection Abrasive Water Jet (iASJ) that utilizes a slurry mixture made mainly of abrasive and water, instead of dry abrasive-particles as used in AWJ, allowing the use of small particle-sized abrasives. To this extent, this work investigates a multi-stage approach using AWJ and common Garnet as abrasive for the first step, and iASJ done with very fine Aluminium oxide abrasive for surface finishing. Before the main experiment, several investigations are done with the goal of improving variables for the final trial, such as jet stability, abrasive settlement time, jet shape and slurry flow-rate. After the process input variables are defined, seven trials are made, considering the main goal of comparing surface quality between a base roughed and a finished test-piece. At the end, results obtained are presented first as a comparison and later as a general view. The work not only shows promising results with the additions made to the setup, but also concludes that a multi-stage approach can indeed be feasible and can bring improvements of more than 10% when milling with slurry-jet at medium-to-high concentrations of abrasive and higher traverse speeds.

Keywords: Slury-Jet. Multi-stage Milling. Surface Finishing.

RESUMO

Alguns métodos convencionais de fabricação, como os que utilizam fresas, não são facilmente aplicáveis quando trata-se de materiais muito duros e quebradiços ou quando eles são termicamente sensíveis. Nesses casos, o uso de métodos não convencionais, como o Jato de Água Abrasivo (AWJ) e suas variações traz alguns benefícios. A fresagem com Jato de Água Abrasivo ainda tem vários pontos a serem aprimorados. Há também diferentes abordagens disponíveis para o tipo de jato utilizado, como o Jato de Lodo Abrasivo injetado (iASJ), que utiliza uma mistura de slurry composta principalmente de abrasivo e água, em vez de abrasivo seco como utilizado com AWJ, permitindo o uso de abrasivos com partículas pequenas. Nesse sentido, este trabalho investiga uma abordagem de vários estágios usando AWJ e Garnet como abrasivo para a primeira etapa, e iASJ feito com abrasivo de Óxido de Alumínio de gramatura pequena para o acabamento da superfície. Antes do experimento principal, várias investigações são feitas com o objetivo de melhorar as variáveis para o teste final, como estabilidade do jato, tempo de assentamento do abrasivo, formato do jato e taxa de fluxo de lodo. Depois que as variáveis de entrada do processo são definidas, são feitos sete testes, considerando o objetivo principal de comparar a qualidade da superfície entre uma peça de teste apenas com desbaste e uma peça de teste com finalização. No final, os resultados obtidos são apresentados primeiro como uma comparação e depois como uma visão geral. O trabalho não apenas mostra resultados promissores com os acréscimos feitos à configuração, mas também conclui que uma abordagem de multiplos estágios pode se mostrar de fato viável e pode trazer melhorias de mais de 10% ao fresar com jato de lodo em concentrações médias a altas de abrasivo e velocidades de avanço mais altas.

Palavras-chave: Jato de Lodo. Fresamento de Múltiplos Estágios. Acabamento de superfície.

LIST OF FIGURES

LIST OF FRAMES

LIST OF TABLES

LIST OF ABBREVIATIONS AND ACRONYMS

AWJ	Abrasive Water Jet
CAD	Computer Aided Design
CAM	Computer Aided Manufacturing
CDM	Controlled Depth Machining
CNC	Computerized Numerical Control
iASJ	Slurry Injection Abrasive Water Jet
MRR	Material Removal Rate
PWJ	Plain Water Jet
SAWJ	Suspension Abrasive Water Jet
TBC	Thermal Barrier Coating
YSZ	Yttria-stabilized Zirconia

CONTENTS

1 INTRODUCTION

Conventional manufacturing methods are in some scenarios not well suited to process the high-performance materials necessary to produce high-tech products, due to their specific characteristics (AXINTE, D. A. et al., 2014). Different from non-conventional processes, they require mechanical contact between the tool and the workpiece (GROTE; ANTONSSON, 2009). Biomedical and Energy-generation sectors make use of high-performance materials, like Zirconium Dioxide (Zirconia), also in combination with the use of non-conventional manufacturing processes (EMELOGU et al., 2016).

One of a such, Abrasive Water Jet (AWJ) Machining has a high cutting performance with comparable advantages to other processes, the ability to machine brittle and ductile materials at very low process temperatures, and versatility when creating complex shapes (GROTE; ANTONSSON, 2009). Because Zirconia is considered brittle, it is highly compatible with usage of AWJ Machining (DESMORAT; LEMAITRE, 2001). Commonly used for cutting, AWJ can also be used for milling, promoting a higher surface quality than some conventional milling methods (GROTE; ANTONSSON, 2009).

Still, non-conventional manufacturing methods lack tailored technologies, such as Computer Aided Design (CAD) and specially Computer Aided Manufacturing (CAM), tools mainly developed to be used with conventional methods (BERGS et al., 2019). Another problem faced when using AWJ Milling is the high number of process input variables, which increase the setup complexity (GROTE; ANTONSSON, 2009). Predicting results of AWJ Milling processes is also difficult, evidenced by the numerous works employing simulation techniques (KLOCKE et al., 2018; ZENG; KIM, 1996; SRINIVASU; AXINTE, D., 2011; RAMESH; MANI, 2022).

Several experiments are done at the beginning in order to achieve a stable output with specific process input variables. Considering the stated difficulties, this study utilizes Slurry Injection Abrasive Water Jet (iASJ) in order to decrease the drawbacks commonly existent in AWJ, allowing the use of finer abrasives and additives in the process (MOMBER; KOVACEVIC, 1998). A multi-stage approach is applied as a way to take advantage of the characteristics of each jet and improve the machining quality with a special configuration, milling the chosen ceramic material with a standard AWJ, and finishing using iASJ.

The use of iASJ in this work help to further characterize AWJ Milling processes. The adoption of multiple stages reinforces the possibility of using two different AWJ approaches, focusing on their unique advantages. Improvement in Surface Quality when compared to AWJ demonstrates to be an important characteristic of the use of finer abrasive particles, possible when using slurry. Nonetheless, the need for low-humidity in the abrasives is discarded when using slurry instead of common AWJ.

1.1 GOALS OF THE WORK

The goal of this work is to investigate the feasibility of multi-stage slurry-jet milling of ceramics. iASJ is firstly considered as the center of study for improvement, focusing on selected process variables. A multi-stage approach is then adopted to investigate surface quality. For this reason, a block of Zirconium Dioxide (ZrO_2) was used as the main test-piece material. At the end, the feasibility of using such technique is evaluated as a combination: Multi-stage slurry-jet milling of ceramics.

Divided into specific goals, then they are:

- Select process input variables in order to improve jet stability.
- Investigate effects that selected abrasives and additives have on the slurry.
- Compare surface quality in pieces processed with use of AWJ and iASJ in a multi-stage milling process.

1.2 DOCUMENT OUTLINE

The document is divided into four more chapters, after Introduction. They are listed with a brief description:

- **Chapter 2 - Bibliographic Review:** Gather fundamental knowledge necessary for general understanding of the next chapters and the work.
- **Chapter 3 - Materials and Methods:** Describes the tools and knowledge necessary to conduct the experiments, before presenting the procedures taken in each one.
- **Chapter 4 - Results and Discussion:** An entire chapter presenting findings from the trials done, described in the previous chapter.
- **Chapter 5 - Conclusions and Future Work:** The thesis finishes, highlighting the main findings and suggesting future work opportunities.

2 BIBLIOGRAPHIC REVIEW

This chapter brings a general view of important topics related to milling and cutting with water jet. Later, it will be explained about the materials chosen for this study and the motivation for those choices, such as their use on general applications. A connection between these topics is made at the end.

2.1 ABRASIVE WATER JET CUTTING

Abrasive Water Jet (AWJ) Cutting is well-known in the industry for the great processing of special materials. Its specific characteristics can be used, for example, as an alternative for a bandsaw, even producing a very similar high-quality cut. Many advantages are due to its high cutting performance, absence of heat in the cutting mechanism and flexibility of the tool. (GROTE; ANTONSSON, 2009).

Compared to other processes, cutting and removing material with a jet of water is known as a non-conventional manufacturing process with a non-defined tool edge. This explains the existence of unusual variables, such as the ones related to the forces applied during material-removing actions and the ones that describe the tool and tool path. The separation between conventional and non-conventional also consider the way of material removal and the type of energy employed in doing so: Mechanical, thermoelectric, electromechanical, and combinations (GROTE; ANTONSSON, 2009).

Most of the process of Water Jet Cutting use some sort of Computerized Numerical Control (CNC) to perform machine movement, that is essential when controlling the Material Removal Rate (MRR) is desired. The Material Removal Rate (MRR) is one of the process output variables that can be measured in order to describe what effects the milling process have into the milled material, and is a time-critical variable (GROTE; ANTONSSON, 2009). The next sections will comment on processes in which the use of a CNC is completely required.

Apart from CNC, other important configurations of the machine are possible when assembling the jet-head. Figure 1 shows the different parts that can be changed to control some machine variables. The complete assembly has important parts apart from the mixing chamber. The water jet orifice can be changed as to control the water-jet pressure. The focusing tube mainly defines the jet-size, but also influence the jet pressure and the abrasive sucking pressure (GROTE; ANTONSSON, 2009).

Surface quality phenomena affect the process directly, as with Waviness and Roughness values. Striation marks happen in AWJ processes and can be minimized by mainly improving the quality of the tool path program, this effect is described by a curved line shown in the surface where the material was removed while cutting. A simple example of it being formed is in Figure 2. The effect can be controlled, in one way, by changing the traverse speed (MOMBER; KOVACEVIC, 1998).

Figure 1 – Jet head assembly composed by many interchangeable pieces.

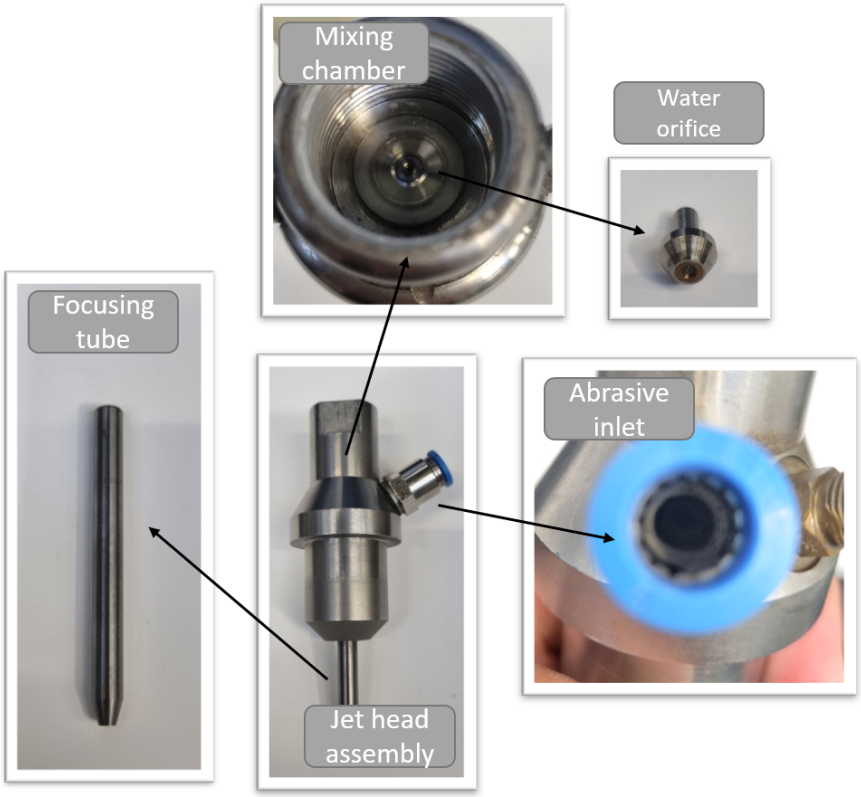

Source: Own authorship.

2.2 PLAIN WATER JET

Pure Water Jet or Plain Water Jet (PWJ) is described by the use of AWJ without any abrasive being injected to the mixing chamber, and it is commonly used to process very specific types of materials that are considered very soft, ductile or sensitive. It can also be used for cutting materials containing a certain degree of mechanical instabilities, such as cracks, micro-cracks and pores (MOMBER; KOVACEVIC, 1998).

The use of pure water with high pressures is shown to be useful in a diverse range of applications for selectively removing a material from multi-composites, such as ceramic thermal barriers (BERGS et al., 2019) or bonded coatings, even with different approaches for the machining path in order to get better results (SANCHEZ; AXINTE, Dragos; SMITH, 2020). These approaches are less related to cutting and more to milling processes, which will be the focus during the next sections.

Figure 2 – Striation forming in an AWJ Cutting process. Striation is influenced by the traverse velocity (v) and its format is described by the depth of cut (h) and the striation size (s).

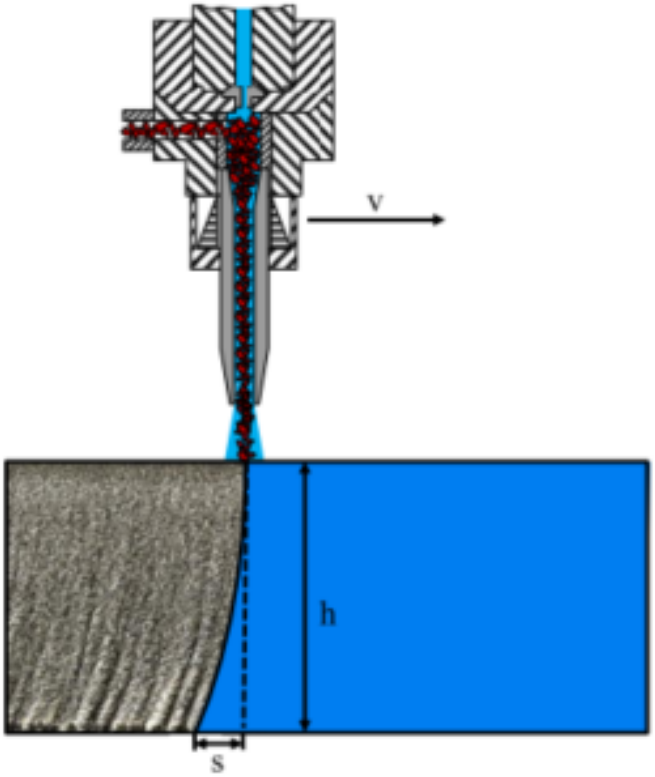

Source: (DADGAR et al., 2021)

2.3 ABRASIVE WATER JET MILLING

Abrasive Water Jet (AWJ) Milling, also called Controlled Depth Machining (CDM) is a modified approach of the AWJ Cutting previously presented. It aims not to cut through the material, but only remove a controlled amount using the jet (MOMBER; KOVACEVIC, 1998).

This method enhance some drawbacks present with AWJ. As the jet is normally composed by three phases (water, air and abrasive), its instability can be a real trouble-maker in some cases. Achieving a stable and continuous jet may also be a difficult task depending on the type being used in the process. In standard AWJ air can constitute up to 90% of the jet-composition in some cases (MOMBER; KOVACEVIC, 1998). Another study observed the existence of different phases on AWJ and the influence caused by the jet composition in material-removal mechanisms, summarizing that a jet with less air, will change the machining characteristics and the effect in the material (BERGS et al., 2020).

The diverse inputs and outputs variables of a process like this can be listed as

is in Frame 1. They are grouped between five main parameter types, such as the ones defined in the machine itself, and the material-specific, as is the case for the abrasive and the material being processed. In the other hand, output variables such as the surface roughness and waviness are influenced by the input ones. A more detailed list of those are presented in Frame 2.

Frame 1 – Input variables for a process of AWJ.

1. Hydraulic parameters	Water pressure Focusing tube diameter
2. Cutting parameters	Nozzle traverse speed Number of passes Standoff distance Impact angle
3. Mixing and acceleration parameters	Nozzle diameter Nozzle length
4. Abrasive parameters	Abrasive mass flow rate Abrasive particle diameter Abrasive particle size distribution Abrasive particle shape Abrasive particle rate
5. Target material parameters	Flow strength Hardness Elastic modulus

Source: (MOMBER; KOVACEVIC, 1998).

Frame 2 – Output variables for a process of AWJ.

Kerf characteristics	Surface Roughness Surface Waviness or Striation Kerf width and taper Burr formation Depth of cut
Accuracy	Geometrical and dimensional accuracy
Material removal	Material removal rate

Source: (MOMBER; KOVACEVIC, 1998).

It is also important to cite the lack of tools to generate proper CAM programs for AWJ Milling processes. Therefore, the function for a milling operation is normally used (BERGS et al., 2019). This increase the complexity in creating solutions that consider AWJ.

2.4 SLURRY INJECTION ABRASIVE WATER JET

Slurry Injection Abrasive Water Jet (iASJ) is a modification to the commonly used AWJ type, being described by the injection of a liquid mixture in the mixing chamber, instead of dry abrasive. The injected mixture normally is composed by abrasive, water, and other additives - such as thickeners - that may be found to be necessary for the process. This mixture is called slurry or in some cases suspension. This approach opens a wide range of possibilities to material processing with a different type of abrasive sizes. With the normal way of feeding abrasives to the mixing chamber, a threshold is created that does not allow for too fine abrasives to be sucked, as they easily clog up the feeding tube (MOMBER; KOVACEVIC, 1998).

Figure 3 shows a common AWJ setup. In the common application, dry abrasive is sucked via the inlet, due to the low-pressure created inside the mixing chamber. In the modified version that iASJ is, the inlet is simply plugged into a slurry tank, so the system sucks slurry instead of dry abrasive.

Figure 3 – Common setup idealized for an AWJ system. The abrasives enter the mixing chamber via an inlet and come off as a slurry jet via the focusing tube orifice. The setup moves with a set traverse velocity in one axis (x), or more.

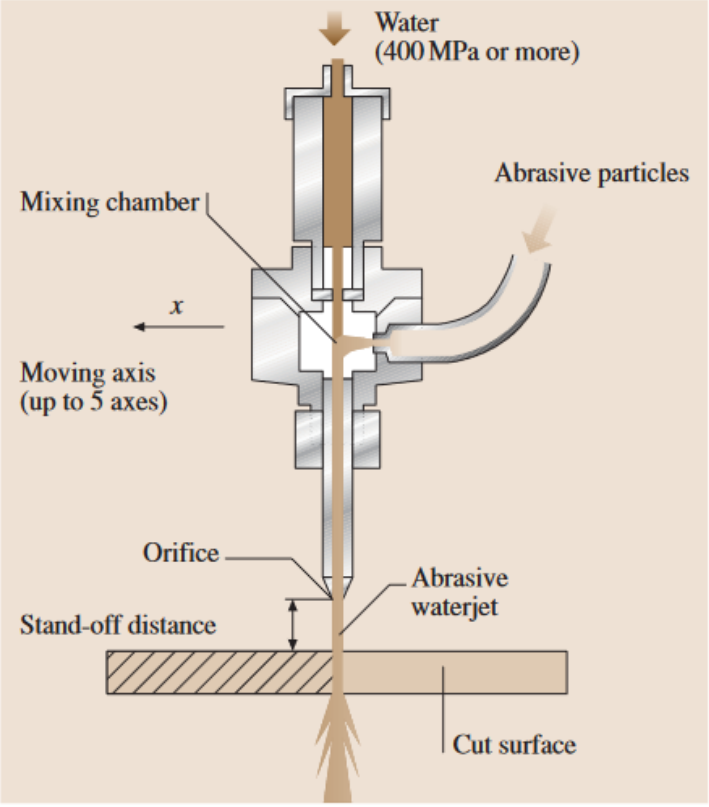

Source: (GROTE; ANTONSSON, 2009).

Another advantage of this approach is the easier achievement of a stable jet, ex-

plained by the existence of almost only two states inside the mixing chamber (water and the liquid mixture with abrasive). The air is present in very little quantities, as demonstrated by previous investigations (TAZIBT; PARSY; ABRIAK, 1996) and explained in depth in the literature (MOMBER; KOVACEVIC, 1998).

Previous works done in the field also focused on applications for finishing and improving surface quality, very likely indicated by the huge benefit of allowing the use of fine-grained abrasives. Different approaches were taken, such as using multiple passes with high pressures and very high concentration of abrasives (HAGHBIN et al., 2015).

Some authors also described multi-stage processes for surface polishing (K.G.; L.; N., 2019), adopting different mixtures and milling approaches in each step, justifying the use of more than one stage to get the required quality as a result.

Changing the viscosity of the slurry with different additives is also investigated in other work (KOWSARI et al., 2014). The tests done show little changes on the geometry of the milled piece even after the use of additive. This indicates that additions to the mixture, such as thickeners, may not affect values related to MRR or to the machined piece profile.

Other authors also conduced experiments with different types of abrasives in materials such as ceramics (KOWSARI et al., 2017) and glass (NOURAEI et al., 2016), showing points to be considered and improved in a iASJ setup. The two materials studied in them were the chosen ones to be used along the experiments presented in this work.

2.5 SUSPENSION ABRASIVE WATER JET

Suspension Abrasive Water Jet (SAWJ) consist of a pressurized mixture used as the jet, this method may also be called just Slurry Abrasive Water Jet, but the main difference between SAWJ and iASJ is the way the slurry is idealized to be used as a jet. On the first one, the mixture of water and abrasive is ready and stored in a chamber, pressurized before going through the output nozzle, in the second one, it is injected in the mixing chamber (MOMBER; KOVACEVIC, 1998).

Compared to AWJ and iASJ, this approach presents a different jet head, this time without the presence of a mixing chamber with inlet for abrasive injection. With SAWJ, the jet head is simpler, as it is only needed to focus the pre-done mixture. Figure 4 exemplifies the many differences between AWJ and SAWJ also when it comes to jet-composition.

Systems that are capable of mixing the slurry inside the pressurized chamber, are called Continuous Suspension type system, here, a complex system mix the slurry without stopping the jet in order to be refiled. This method of creating the abrasive jet has several advantages compared to AWJ, such as the extreme stability and the possibility of using abrasives of smaller grain-sizes, just as in iASJ (PUTZ et al., 2018).

Figure 4 – Comparison between an AWJ and a SAWJ system setup. Both have an inlet for pressurized water (P_pump) that enters the setup with a given pressure (P_w). Abrasive enters the setup with particle mass (M_p) and is accelerated with velocity (V_w). The setup is normally configured with a specific focusing tube orifice size (D_i or D_s) and a set stand-off distance (s).

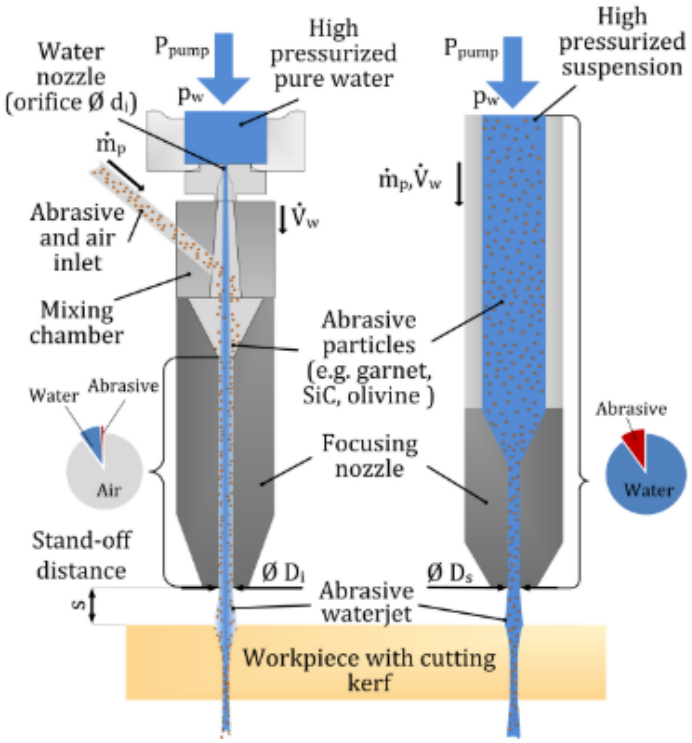

Source: (PUTZ et al., 2018)

Some research done in the area, described and evaluated the approach, indicating that it has advantages when comparing the results with other jet-system like AWJ (PUTZ et al., 2018). Studies also done with composites concluded that the presence of air in the jet, as happens in AWJ, create drawbacks related to the quality or material removal, minimized in SAWJ (RAMESHA et al., 2019). Some negative points are the accelerated wear and tear of the focusing tube, and the high price and necessity of maintenance of the equipment, additionally affected by the fact that it is a recent technology (MOMBER; KOVACEVIC, 1998).

2.6 ABRASIVE AND SLURRY MIXTURE CHARACTERISTICS

Abrasives are chosen to be used on a process based on several material-specific characteristics and also on the piece in which they will cause an impact. Either sieving the grains or selecting a specific grain-size or mesh-size directly from the supplier is also necessary, as considering it is critical for the process.

The most used abrasive material for AWJ applications nowadays is Garnet,

one of the two being used on this study, the other is Alumina (Al_2O_3). To cite other possibilities to chose from, two main groups exist, one is the oxide group, with materials like magnetide, ilmenide, corundum, rutile and quartz as subgroups. The other is the silicate group, containing abrasive materials like Garnet and other kind of silicate as subgroups (MOMBER; KOVACEVIC, 1998).

A study categorized the influence that some abrasive properties have on erosion in AWJ Machining (SCHÜLER et al., 2021). The authors selected three types of abrasives with different geometries and material compositions, two spherical-shaped and one angular-shaped. Shape and size of the grain directly impact aspects such as surface roughness and MRR. The round or angular particles can produce smoother or rougher surfaces, respectively. During the process, angular shaped particles remove material easier than spherical ones, very likely due to their sharp edges (MOMBER; KOVACEVIC, 1998).

2.7 MATERIALS AND EROSION MECHANISMS

Two main materials were used for being machined during the experiments of this study, the first one is Glass (SiO_2) and the second one is called Zirconium Dioxide (ZrO_2), also known as Zirconia, not to be confused with Zircon ($ZrSiO_4$) which has different properties and was not used in this work. Glass and Zirconia both typically exhibit high strength, high hardness, high elastic modulus, unusually high chemical inertness, and are electrical and thermal insulators (DANTE, 2016).

Several mechanisms cause removal of material in the process of AWJ Milling, they are presented in Frame 3. In the case of materials like Zirconia and Glass, mainly in the form of fracturing, crack formation and finally disruption (MOMBER; KOVACEVIC, 1998). Both materials used in the experiments are considered brittle materials because they have extremely low plasticity, in which cracks can initiate without plastic deformation and can soon evolve into brittle breakage (DESMORAT; LEMAITRE, 2001).

Frame 3 – Erosion mechanisms caused by solid particle impingement.

Cutting	Penetration of Cutting Edge Plastic Deformation to Failure
Fatigue	Cyclic Failure
Brittle Fracture	Non-Cyclic Failure
Melting	Loss of Fluid State

Source: (MOMBER; KOVACEVIC, 1998).

Zirconia was chosen to be the studied material based on the way AWJ effect materials with its characteristics. Unlike the ones such as metals and composites, Zirconia also narrows the scope of study in the list of possible erosion mechanisms as

it has high strength and hardness, and material removal happens mainly in the form of fracturing (MOMBER; KOVACEVIC, 1998).

2.8 APPLICATIONS OF ZIRCONIA

In the Biomedical sector, special materials like Zirconia are widely used in prothesis because of its characteristics. The presence of pores in the material and its high-strength are some of the main reasons why it is used. Previous studies show that those are indeed applicable for this area, depending on the needs presented by each manufacturing approach (EMELOGU et al., 2016).

At the energy industry, Thermal Barrier Coating (TBC) for several types of applications due to the high heat-resistance needed. Steam turbine blades can be made out of Zirconia, as the one shown in Figure 5. More specifically, this type of coating is made with Yttria-stabilized Zirconia (YSZ), with very similar properties to the Zirconia type used in the experiments (MOMBER; KOVACEVIC, 1998).

Figure 5 – Turbine blade with partially removed TBC made of YSZ.

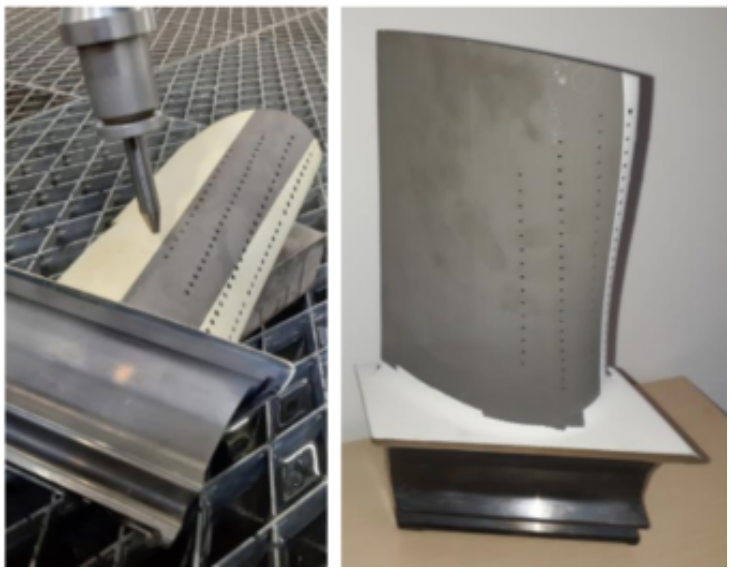

Source: (BERGS et al., 2019)

3 MATERIALS AND METHODS

Firstly, in the Materials and Methods chapter, the main tools used in order to realize the experiments are presented. After, the following sections describe the methods adopted to achieve the first goals of having a stable system, and then, to process the test-pieces as to investigate the feasibility of multi-stage slurry-jet milling of ceramics.

The end of the chapter focus on the methodology, fixed variables are defined, based on the results obtained from primary experiments. Methods are discussed alongside this part of the work, but the results will be deeply presented and discussed in Chapter 4.

3.1 ORIGINAL EQUIPMENT

The equipment is constituted mainly by a Water-jet Cutting Machine *H.G. Ridder* type WARICUT E-11045 Micro-max (RIDDER, 2023) equipped with a Siemens Sinumerik 840D CNC (SIEMENS, 2023) with five-axis of freedom, limited by the dimensions of 795 mm on the X axis, 745 mm on the Y axis and 440 mm on the Z axis. The travel limits of the rotational axes A and B axis are of +/- 540 and +/- 95 degrees respectively. A first view of the machine is shown in Figure 6. An ultra-high-pressure pump by *ThyssenKrupp-Uhde* type HPS4022-OEM (THYSSENKRUPP-UHDE, 2023) is used in the water pressure system of the machine. It promotes pressures of up to 400 MPa (4000 bar), using a double-plunger piston.

Figure 6 – Side-view of the machine.

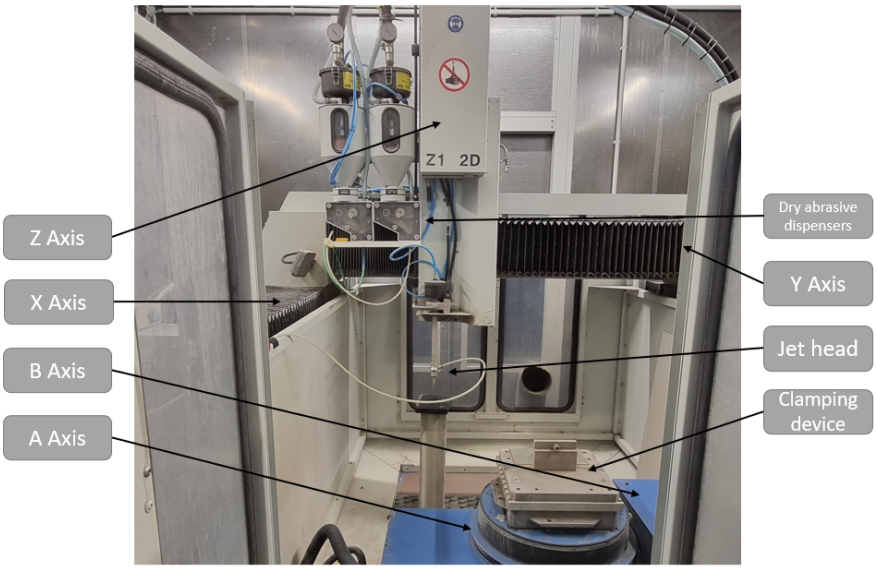

Source: Own authorship.

A vise was also set into the machine in order to hold the test-pieces. Figure 7 present a close-up view of the setup that hold the pieces. Protective pieces of metal were also inserted at the sides in order to protect the equipment from the jet deviating from the aimed piece.

Figure 7 – Clamping vise attached to the machine. A glass test-piece is placed into it.

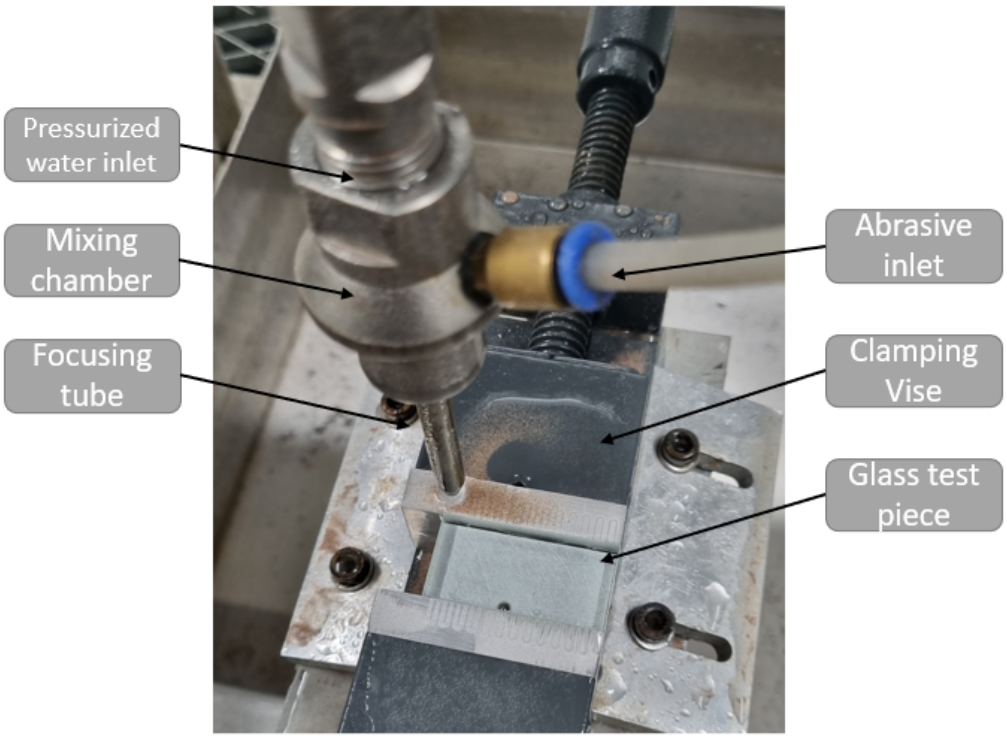

Source: Own authorship.

3.2 OTHER EQUIPMENTS AND TOOLS USED

Not only the AWJ CNC machine was important for the experiments, but with the final experiments, a deep analysis of the milled material should be possible. Common microscopes can only generate a 2D view of a piece, requiring the use of one capable of making a 3D analysis. 2D microscopes were initially used for quick inspections and to capture pictures. Initial experiments, that would define machine-related variables, needed to be re-done a couple of times, so the simplicity of a tool like it came in handy.

For complex analysis such as 3D-surface-profiling, it made necessary the use of tools like *Alicona InfiniteFocus G4* (ALICONA, 2023), showed in Figure 8. It generates a profile of the surface based on image capturing and varying its focus during the measurement. With the high-fidelity model created by the tool, values like surface roughness and waviness could be measured.

Figure 8 – Alicona InfiniteFocus G4.

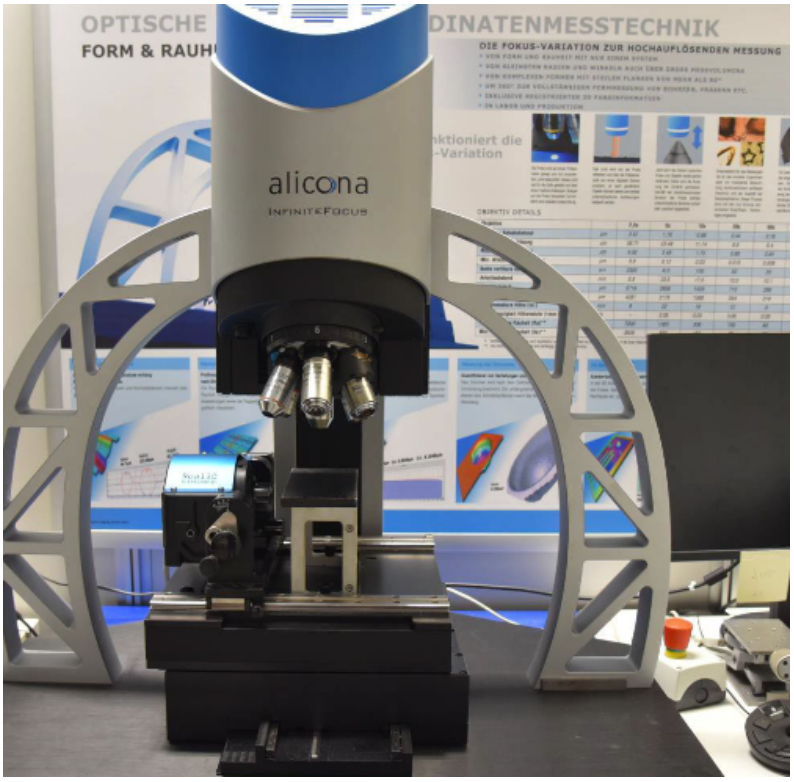

Source: Own authorship.

Software products like *MATLAB* (MATHWORKS, 2023) and *MountainsLab* (SURF, 2023) were employed to process the output 3D-point-cloud generated with the use of Alicona. Initial experiments used a code programmed in MATLAB that generate a report containing the desired variables. In later experiments, the surfaces of the test-pieces contained smaller differences that prevented to continue using MATLAB, so the use of MountainsLab was adopted. In both cases, the same variables for surface analysis were considered.

Other tools like a vibrating sieving-machine and an ultrasonic-cleaning machine were employed to other jobs that not inspect the test-pieces, examples of their use are illustrated in Figure 9. The sieving had to be done to separate the desired grain-sizes of abrasive, sieves of mesh-size 150 and 200 were the main ones used. For finer abrasives, no sieving was necessary as they were ordered with the desired grain-sizes directly from the supplier. On the other side, tools like the ultrasonic cleaning was necessary to remove rest of particles left in the milling process done with the test-pieces, this was important to avoid erroneous results in the profile measuring.

Figure 9 – Other crucial tools used on the experiments, machines for sieving (left) and cleaning (right).

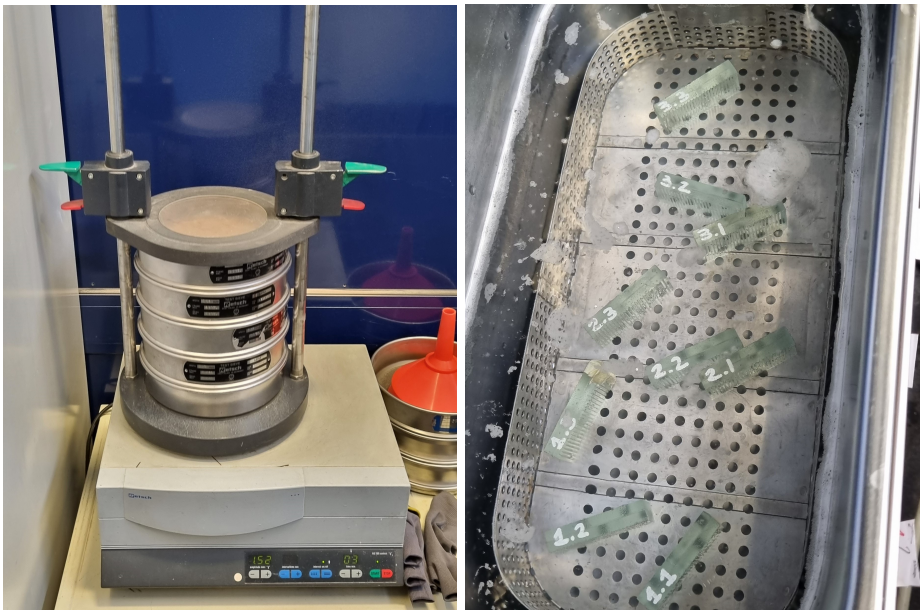

Source: Own authorship.

3.3 PHYSICAL SETUP FOR SLURRY JET MILLING

The original machine is not constructed to directly support milling with iASJ, with a jet-head composition and reservoir intended for dry abrasive. Thus, an apparatus had to be mounted to it to allow injecting slurry in to the mixing chamber. In the top of the setup, showed in Figure 10, there is a beaker with magnetic steering plate that maintained the slurry well mixed during experiments, the equipment also allowed to control the velocity of the mixing action. On the bottom of the steering setup is a weighing scale, employed when slurry flow-rate needed to be measured, this was done with the aid of a chronometer. A hose leaving the glass beaker that would then carry the slurry, passing by a spherical valve that controls the slurry flow-rate entering the mixing chamber.

3.4 SLURRY MIXTURES

Several batches had to be made for each experiment that needed a different type of abrasive or concentration of it. Normally, mixtures would be made in a 500 ml bottle and filled with 400 ml of water from the tap, together with a certain portion of the selected abrasive. In later cases, the experiments adopted the addition of a thickener at the beginning, with a little bit of alcohol so that it avoided creating lumps of powder. The specific material added during the experiments is called Xanthan, and is showed

Figure 10 – Parts necessary to set up slurry injection in the AWJ system.

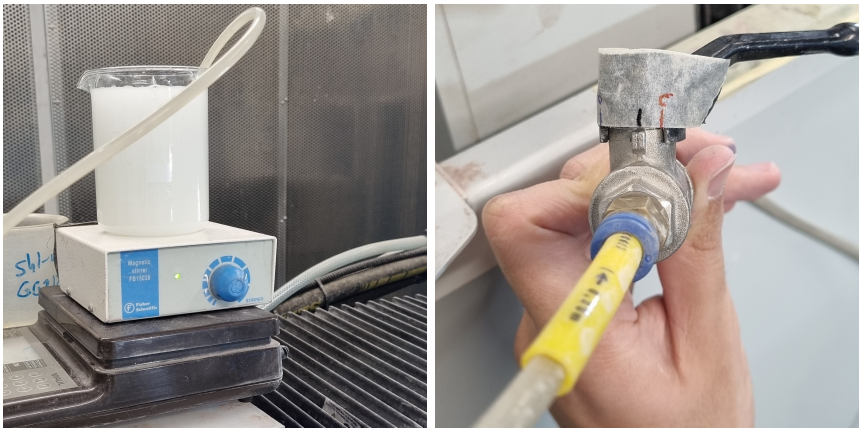

Source: Own authorship.

in Figure 11, but mixtures recipes will be presented on each specific section related to the experiment in which they were used.

Figure 11 – Example of slurry mixture (on the left), containing the thickener (showed on the right).

Source: Own authorship.

3.5 TEST PIECES

Two types of test pieces were used, both showed in Figure 12. On the first experiments, Glass (SiO_2) test pieces were used. This was justified by the low value attached to the part and the nature of the initial experiments, a glass piece would allow seeing any variability on the jet without the need of a microscope. The initial use of glass test-pieces instead of Zirconia ones is possible due to the extreme similarities between

the materials. As described in Chapter 2, both exhibit high strength and hardness, thus have a relatable way of observing the output results.

Figure 12 – Test-pieces used on the experiments. Zirconia (on the left), and glass (on the right).

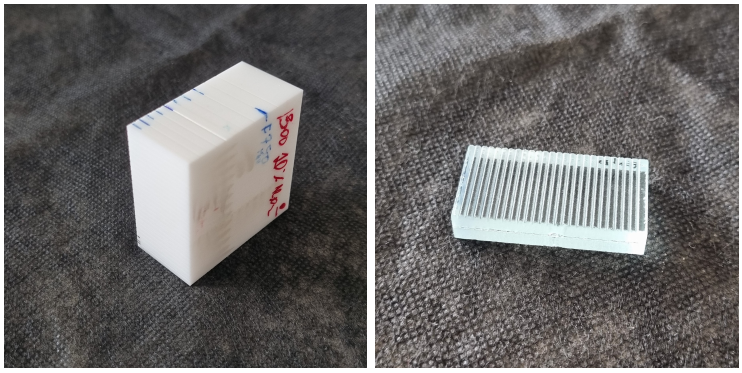

Source: Own authorship.

The glass test pieces were prepared as rectangles cut from a big plate, with size of 20 x 40 mm, the thickness have no influence, as long as it is enough for the deep groves to be made in the tests, the plates used had ten millimeters of thickness. The second test-piece type was a block of Zirconia (ZrO_2). The block had dimensions of 40 x 40 x 20 mm. Those two test-pieces were used later to be processed by the two abrasive types made of Garnet and Alumina.

3.6 CAM PROGRAM CREATION

The CAM program was designed to make 25 lines in one lateral face (of size 40 x 20 mm) of the Zirconia block, each five groups of lines had a set traverse velocity for the jet. It was not necessary to use any type of CAD to create the tool-path, due to its simplicity. This configuration would allow to easily inspect the pieces later as they had a fixed distance between the line.

The five traverse velocities set in the same program were 250, 500, 750, 1000 and 1250 mm/min, respectively for each group. Each line was spaced by 1.5 mm and covered all the length of one side of the block, meaning that only the coordinates X and Y were used. A 2D-view is in Figure 13, the G-code used for generating it is also available on Appendix A. The entire program took one and a half minute from start to finish.

3.7 PRIMARY EXPERIMENTS

The primary experiments are presented in this section, as a better way of organizing the Methodology and the Results. It is separated into seven subsections, each

Figure 13 – Top-view of the tool-path generated with the code. Each group of five lines is configured with a different value for traverse speed.

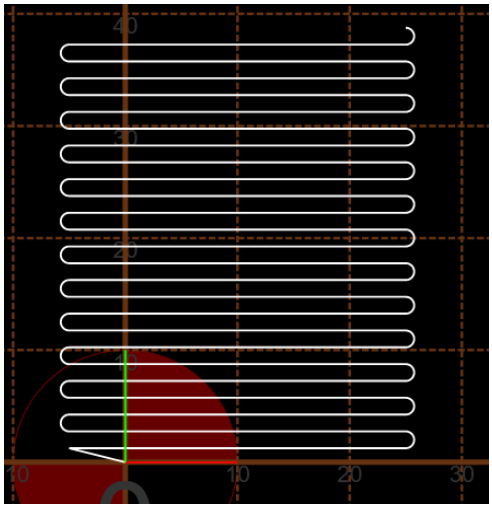

Source: Own authorship.

one describing the approach to a different experiment that at the end would help define the main experiment.

3.7.1 Machine Variables setup

Milling with AWJ has the drawback of having many input variables. As a way to focus the scope of the research, this work considered changes in some of them, such as Water Pressure and the ones related to Abrasive. Frame 4 group the main variables considered to the experiments, with a brief description of what it is. The process is mainly influenced by the water pressure, the abrasive concentration, and the traverse velocity.

Variables that were initially defined as constant along the experiments, are presented on the Frame 5, and are considered for every other experiment that follow in this chapter. As a way of reducing the number of choices and combinations to make, they were set based on previous works done by others authors such as with slurry (HAGHBIN et al., 2015) or in a multi-stage approach (K.G.; L.; N., 2019). The orifice and focusing-tube diameters were chosen based mainly on the set of abrasives that were going to be used in the experiments, as to avoid clog ups.

The other variables set in later experiments also take into consideration previous studies done by other authors, but as each did a different set of them, their methodology only served as a guideline. The time-frame available for executing the experiments also had to be taken into consideration.

Frame 4 – Machine parameters utilized along the work.

Orifice Diameter (mm)	Diameter of the jet created inside the mixing chamber.
Focusing Tube Diameter (mm)	Diameter of the focusing tube.
Standoff Distance (mm)	Distance between jet nozzle and workpiece.
Impact Angle (°)	Angle from the jet-nozzle and the workpiece.
Water Pressure (bar)	Water pressure defined on the pump.
Thickener Concentration (g/l)	Concentration of thickener used on slurry batches.
Abrasive Size (µm) or Abrasive Mesh-size (#)	Abrasive grain-size.
Abrasive Type	Material-composition of the abrasive.
Abrasive Concentration (%)	Concentration of abrasive in the slurry.
Abrasive Mass-flow (mg/min)	Concentration of abrasive being injected into the mixing chamber.
CNC Program Used	CNC program used to run the tests.
Traverse Velocity (mm/min)	Transversal velocity of the nozzle.

Source: Own authorship.

Frame 5 – Machine parameters adopted for all the experiments.

Orifice Diameter (mm)	0.12
Focusing Tube Diameter (mm)	0.54
Standoff Distance (mm)	2
Impact angle (°)	90

Source: Own authorship.

3.7.2 Slurry flow-rate

The need for measuring the slurry flow-rate is justified by the need of estimating the behavior of MRR, this can be done by calculating the amount of abrasive entering the mixing chamber, as a flow-rate, in the case of slurry. Four set of experiments were done, each one with a different slurry viscosity, the first having only water. At the end, flow-rate was calculated as a function of the mass and the time. This would also allow calculating the abrasive-flow-rate in the next experiments, as the concentration would be known.

The first experiment was conduced with only water and other three slurry mixes with of 0.75, 1.5, and 2.25 grams of thickener per liter of water. Frame 6 summarize the

variables used on this experiment, CNC-related variables are not present, as everything was done without any machine movement or material. The results will be discussed in the next chapter.

Frame 6 – Variables used for the slurry flow-rate experiment.

Water Pressure (bar)	750; 1000; 1500; 2000
Thickener Concentration (g/l)	0; 0.75; 1.5; 2.25

Source: Own authorship.

3.7.3 Jet-shape Measurement

Investigations regarding the shape of the jet that left the focusing tube were also done in order to observe changes caused by the insertion of different mixtures of slurry into the mixing chamber. The idea of evaluating the jet-shape using computer vision was a step-up in the analysis promoted in this study. As it could be done without much need of further equipment, it would be completely viable as a prototype and first application for measuring the effects caused by different slurry mixtures in the jet-shape of iASJ. This was inspired by the measurement done in a related work (HAGHBIN et al., 2015) that also idealized iASJ, the main difference is that the author measured using a piece of Styrofoam instead of using computer vision and pictures.

The pictures were taken during the Slurry flow-rate experiment described in the previous section, so the machine variables considered should be the same. Figure 14 shows one of those pictures taken in the duration. The main idea was to investigate if the addition of *Xanthan* as thickener would change the jet-shape and perhaps affect the iASJ milling process.

The jet-shape measurement method adopted used computer vision with the help of tools like Python and OpenCV (OPENCV, 2023). The algorithm developed calculated widths in order to characterize the jet-shape. At the end, the algorithm also generated an image containing the analysis and an output table containing the measurements. The code is also available in Appendix B.

The algorithm works following the steps:

- Apply a binary-filter to the image in order to highlight the jet.
- Highlight the area of interest of the jet, removing splashes and spills.
- Measure the width of the jet in some points.

3.7.4 Abrasive Settlement Time with Thickener

In order to characterize the effects that thickener could have in the mixtures, some batches were made and pictures were taken with set intervals in order to observe

Figure 14 – Example of photo take in order to measure the jet-shape.

Source: Own authorship.

the settlement time of the abrasive in each one. This would allow making a better decision on how much thickener to put in the slurry mixtures in order to maintain the abrasive in suspension for a longer time.

Figure 15 shows the setup used, it has three pairs of bottles with different thickener concentrations inside. Within, one having a mixture with 0.075 µm grain-sized Garnet abrasive and the other one grain-size 0.106 µm. More about the experiments will be explained in the next chapter, together with the results. Frame 7 summarize the variables used for the mixture combinations.

Frame 7 – Variables used for the abrasive settlement experiment.

Abrasive Size (µm)	0.075; 0.106
Thickener Concentration (g/l)	0; 0.75; 1.5; 2.25

Source: Own authorship.

Figure 15 – Setup for abrasive settlement time analysis using time-lapse.

Source: Own authorship.

3.7.5 Improvement of Jet-stability with Glass Test-piece

The first experiments used only water, which showed to have a narrow window of stability. To investigate further possible solutions, thickener was added to the mixture, just as done in the flow-rate experiments, and then another set of experiments were done to create two curvatures defining the stability characteristics based on the valve position.

The two top and bottom thresholds of stability were set by opening or closing the valve from its fully-closed or fully-open position, and taking note of the position. The position was recorded as a percentage value that describe how opened the valve is. The set pressure over the experiment was 1500 bar, and the slurry initially had no abrasive in its composition.

Improving the jet stability is a crucial step on the experiments, that is why other experiments followed, now with the use of glass test-pieces processed with 1500 bar of water pressure and a slurry mixture containing a 5% concentration of Garnet abrasive with 0.075 µm grain-size, process variables that would remove only enough material from the test-piece so that the jet stability could be visually detected. The pieces were set into the clamping vise and machined with the standard CNC program presented before. The variables for this experiment are also contained in Frame 8.

With the observations done during the series of experiments presented in this

Frame 8 – Variables used for slurry jet-stability experiment using glass test-pieces.

CNC Program used	Yes (standard)
Water Pressure (bar)	1500
Abrasive Type	Garnet
Abrasive Size (µm)	0.075
Abrasive Concentration (%)	5

Source: Own authorship.

subsection, corrections in the previously obtained results were made. A more thorough discussion will be done in a later chapter.

3.7.6 Material Removal with Glass Test-piece

The material removal is an important measurement related to the milling process, it can indicate the quality of the process and, for example, guide the next steps as to which set of variables to go with in the final experiments. These tests were done as a way to visually observe behaviors related to MRR. Glass was used because of its numerous already here-stated advantages and the limited-availability of Zirconia. Experiments of this section were done using iASJ, as from this point on, the work will focus on the use of slurry injection.

The process was divided in three parts, and three groups of test-pieces, the first one was processed with 1000 bar, the second with 1500 bar, and the last with 2000 bar. Inside each, three glass-pieces were milled, the first with 5 % of abrasive concentration, the second with 7.5 % and the third one with 10 %. All the slurry mixtures adopted a quantity of 2.5 g/l of thickener. The Frame 9 bunches together all the variables here described.

Frame 9 – Variables used for slurry material removal-rate experiment using glass test-pieces.

CNC Program used	Yes (standard)
Abrasive Type	Garnet
Abrasive Size (µm)	0.075
Thickener Concentration (g/l)	2.5
Abrasive Concentration (%)	5; 7.5; 10
Water Pressure (bar)	1000; 1500; 2000

Source: Own authorship.

After all the pieces were processed, they were inspected with the use of Alicona, to collect the surface profile. The data was then post-processed using MATLAB and a report was generated containing surface-quality and profile analisys.

3.7.7 Roughing of Zirconia Test-pieces with AWJ Milling

One important preparation for the final experiments is the roughing of some surfaces in the Zirconia block. These process were made with AWJ, using Garnet with a mesh size of 150 (89 µm), 2000 bar of water-pressure, traverse velocity of 500 mm/min and 60 mg/min of abrasive mass-rate. The variables were chosen based on the need of a process with AWJ that would remove a lot of material, and in previous work done (SCHÜLER; HERRIG; BERGS, 2022). Others parameters of the machine were set as usual. The Frame 10 list some important experiment variables.

Frame 10 – Variables used for the roughing of the Zirconia surfaces using AWJ.

CNC Program used	(Modified version)
Traverse Velocity (mm/min)	500
Water Pressure (bar)	2000
Abrasive Mass-flow (mg/min)	60
Abrasive Type	Garnet
Abrasive Mesh-size (#)	150

Source: Own authorship.

Figure 16 illustrates the differences between a surface before and after being processed with the roughing process. The groves created were inspected with Alicona to have comparable data after the finishing process. They had a depth of around 50 nanometers.

Figure 16 – Blocks of Zirconia, before roughing process (left) and after (right).

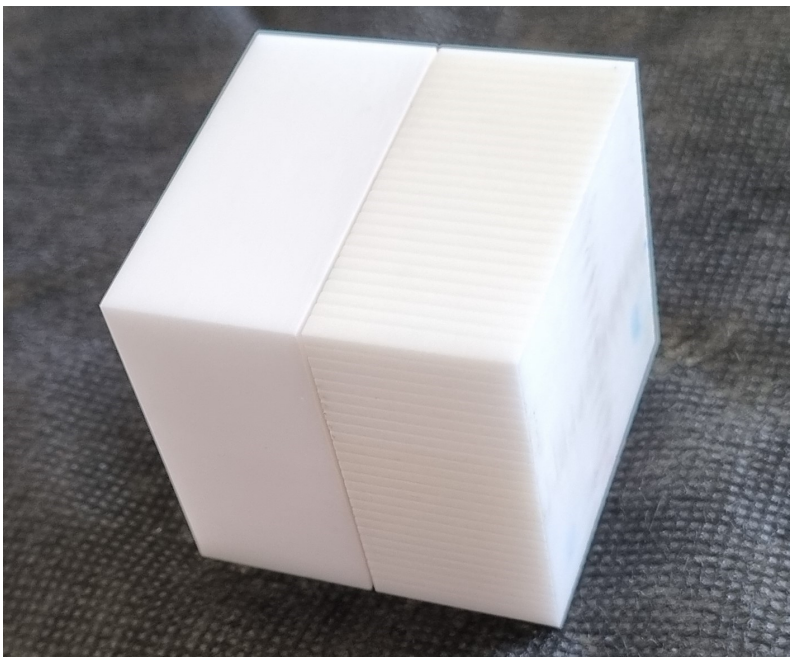

Source: Own authorship.

3.8 MULTI-STAGE PROCESSING WITH ZIRCONIA

The final experiment is presented in this separated section, as its goals are specifically related to the final investigation about the feasibility of multi-stage milling with iASJ. This section presents the method adopted to process the pre-roughed lines in the face of Zirconia.

Seven roughed faces of Zirconia were handled and processed into the machine now with use of iASJ for finishing purposes. The variables were defined based on all the previous experiments done, but mainly in results obtained withing experiments of material removal, done with glass. Based on results from previous experiments, seven abrasive-concentration variations were selected, the Frame 11 contain those variables.

Groups of 25 lines were processed, each one with a different concentration of the abrasive selected for the finishing process. Just as in the last experiment, some variables, such as pressure and abrasive concentration, are justified by results presented in the next chapter, just as a deep explanation of each choice done.

Frame 11 – Variables used for finish-milling Zirconia surfaces with iASJ.

CNC Program used	Yes (standard)
Water Pressure (bar)	1500
Abrasive Type	Aluminia (Al_2O_3)
Abrasive Mesh-size (#)	350
Thickener Concentration (g/l)	2.5
Abrasive Concentration (%)	1; 2.5; 4; 5; 7.5; 9; 10

Source: Own authorship.

4 RESULTS AND DISCUSSION

This chapter aims to show the main results and also bring discussion about what was discovered with each experiment carried. Future work possibilities may be briefly mentioned, but will be mainly approached in the Chapter 5.

Results are presented in two sections, the first focusing on the several results from the initial experiments, done to define all the variables for the final experiment. The second section will approach the results from the final experiments and discuss in depth only this part of the several investigations done.

4.1 PRIMARY EXPERIMENTS

As structured previously in Chapter 3, the numerous experiments realized have each one narrowed into one conclusion, idealized in order to continue with the next. Here in this section, the results are presented in a manner trying to connect each one with its successor.

4.1.1 Slurry flow-rate

As stated, the first step, after defining fixed machine variables, was to calculate the slurry flow-rate. With the results gathered within the experiments section, the once tabular-data was used to calculate values like the flow-rate in milliliters per second (ml/s), with the three values: Initial mass, final mass and elapsed time. As four trials were done with different thickener concentrations, four different graphs were generated, and put together as the Figure 17. This experiment also observed the possible behaviors in order to guide the thickener amount to be used in each slurry batch.

It is notable how in the case in which only water was injected as slurry, the flow-rate rises in function of the pressure. In cases where the slurry had a bit of thickener in its composition, almost the same behavior can be observed, but at higher pressures, the flow-rate stabilizes. In the case of higher slurry viscosity, the results were different, having an almost continuous value. The fourth measurement of the 2.25 g/l thickener concentration is missing due to an incorrect measurement that was discarded.

Behaviors can then be separated into three categories. The first one being what happened with water, where the viscosity is very low. This caused an almost linear increase of the flow-rate related to the pressure, followed by a slow stabilization. The second behavior happens with the slurries done with low-viscosity (0.75 and 1.5 g/l), where there is also an increase of the flow-rate related to the pressure, but it stabilizes with lower pressures than in the case with pure water. The last behavior happen when the slurry is too thick, and causes it to flow with an almost stable flow-rate from start to finish.

Figure 17 – Slurry flow-rate based on thickener concentration.

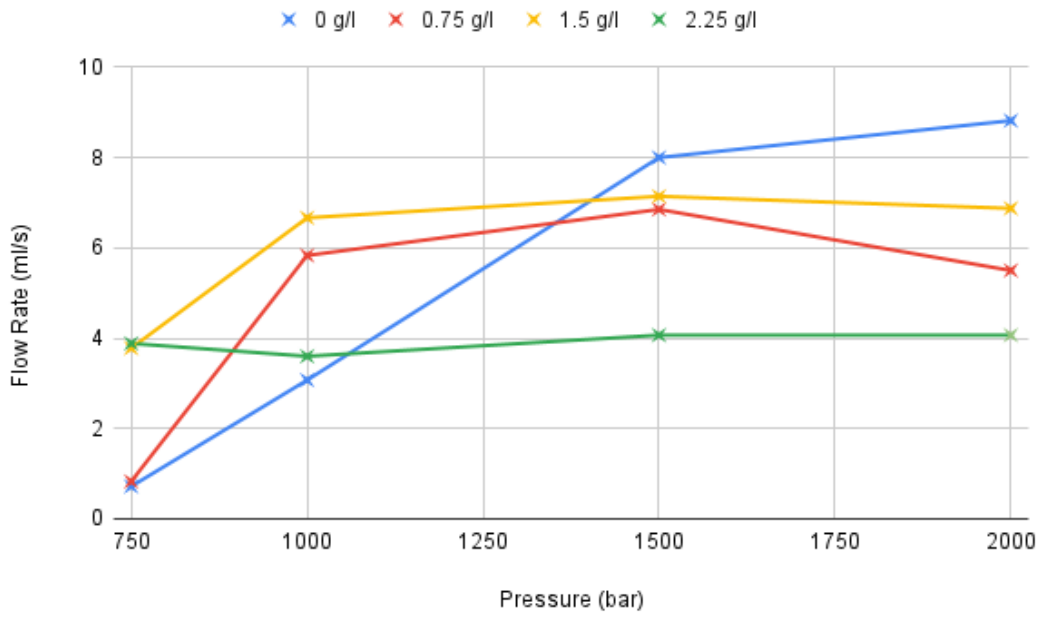

Source: Own authorship.

The graphs indicate that as more thickener is added, increasing the viscosity of the slurry, the flow-rate not only decreases, but also start to stabilize to a fixed value, sooner than when compared to with lower viscosities. With 2,25g/l for example, the flow-rate is the same for all the pressures of water, lower than

4.1.2 Jet-shape Measurement

To help characterize the process, several jet-shape measurements were done with help of a script, at least one for each concentration of thickener experimented. The code used generated composed pictures with the data overlaid on top of the original, the pictures of the four analyzed jet-shapes are in Figure 18.

Further improvement on the way the code works may be necessary when applying to more complex analysis. As each image is slightly different from the other, results would vary a little depending on how the algorithm segmented the jet part and more than only the jet would be caught in the measurements. Table 1 list all the variables gathered with the processing. The measurements here presented were done into three vertical points, starting from the center of the image and each one going 500 pixels upwards from the previous.

Data gathered with the four jet analysis can be analyzed as to characterize the jet-expansion. All the jets have a similarly linear increase in width from the first measurement to the next, in the cases of *Jet 1* and *Jet 2* of around five pixels and

Figure 18 – Slurry-jet images with analysis overlaid on top for better visualization.

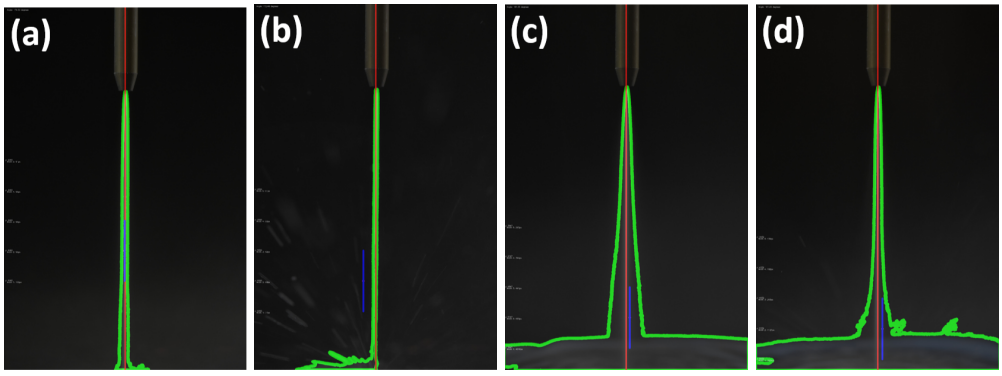

Source: Own authorship.

Table 1 – Jet-shape measurements done in three points along the jet. Jets with thickener concentrations of (a) 0 g/l, (b) 0.75 g/l (c) 1.5 g/l (d) 2.25 g/l.

Identification		**Input Variables**		**Data Measured in the Image**		
Image Name	**Experiment Number**	**Thickener Concentration (g/l)**	**Pressure (bar)**	**Width 1 (pixels)**	**Width 2 (pixels)**	**Width 3 (pixels)**
(a)	1	0	1000	91	96	99
(b)	2	0.75	1000	51	50	62
(c)	3	1.5	1000	263	344	441
(d)	4	2.25	1000	139	182	263

Source: Own authorship.

in *Jet 3* and *Jet 4* of around 85 pixels, indicating that they have a similar increase in size, always very minor. When comparing all the jets, it is visible that no big changes in jet-size happen between each experiment. A little increase may be noticeable when comparing *Jet 1* with 0 g/l of thickener, with the *Jet 4* with 2.25 g/l concentration, but the change is minor and should still not affect the final result, as other variables such as the homogeneity of the jet mixture can cause bigger changes than the ones observed.

4.1.3 Decantation: Abrasive Settlement Time

Measuring the abrasive settlement time was also another step done into the experiments in order to help trace the slurry behavior when thickener was added to the mixture. The main goal was to register the time it takes until the abrasive particles start to settle down. As described in the last chapter, six batches were made and photos taken from time to time. Figure 19 put four frames together, taken respectively after one minute, eight minutes, 36 minutes, and nine hours and 56 minutes after the start of the experiment. The results are better described in Table 2, the values were measured based on how much abrasive was still in suspensions, and obstructing the passage of

light. Values like 0% means that none of the abrasive was settled, almost fully blocking up the passage of light, while 100% means that light could pass through the bottle, meaning no abrasive was in suspension in that area to block it.

Figure 19 – Bottles with slurry mixtures in fours stages of settlement, taken minutes after start: (a) 1 minute, (b) 8 minutes, (c) 36 minutes and (d) 9 hours and 56 minutes.

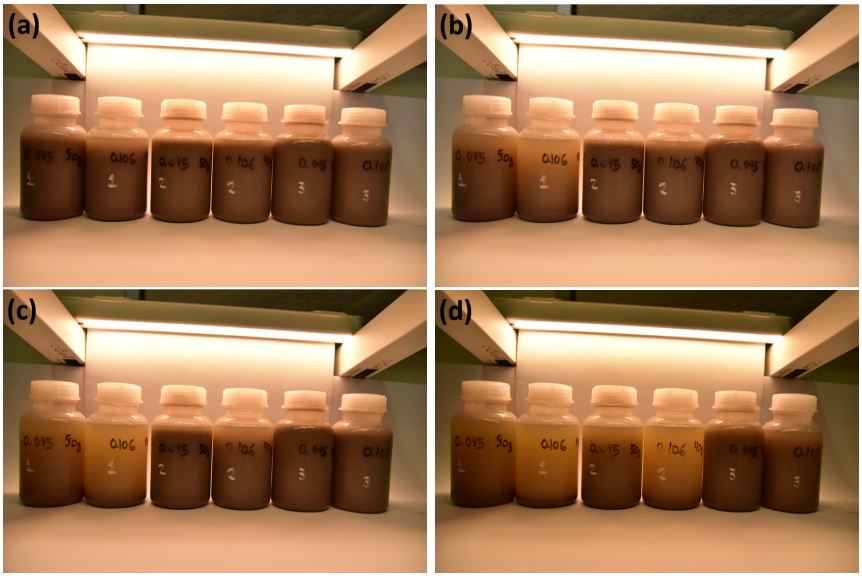

Source: Own authorship.

Table 2 – Settlement observed at specific timestamps for each bottle of slurry mixture.

Naming	**Mixture Composition**		**Settlement Percentage on each Timestamp (%)**				
Bottle	**Abrasive Size (µm)**	**Thickener Concentration (g/l)**	**Timest. 0h0m**	**Timest. 0h1m**	**Timest. 0h8m**	**Timest. 0h36m**	**Timest. 9h56m**
Bottle 1 (left)	0.075	1.2	0	5	25	85	95
Bottle 1 (right)	0.106	1.2	0	10	75	95	100
Bottle 2 (left)	0.075	2.4	0	1	3	5	75
Bottle 2 (right)	0.106	2.4	0	2	5	10	95
Bottle 3 (left)	0.075	3.6	0	0	0	0	5
Bottle 3 (right)	0.106	3.6	0	0	1	1	10

Source: Own authorship.

Results indicate that the addition of thickener to the mixture causes the abrasive settlement time to rise up. After eight minutes, a big amount of abrasive had settled in

the bottle containing the bigger particles and low concentration of thickener. The result observed in the last two bottles (with 3.6% of thickener concentration) demonstrate that it might be unnecessary to use more than 3.6 g/l of thickener, as it took more than ten hours to fully settle. This experiment also served to support the investigation on how the grain-size could influence the experiment, demonstrating that a finer abrasive can stay in suspension for longer than a bigger grain-sized one.

4.1.4 Jet-stability

From all the investigations done until now in this work, jet-stability is one of the most important to be made before the final trials. In this experiment, first a basic test was done without use of any test-piece, in order to create a profile of stability based on the slurry valve-position. Stability was achieved by doing a series of trials with valve positions. Figure 20 describes the jet behavior on each variable explored. The graph contains a red line on the top part that indicates the maximum valve opening before achieving instability. The blue line bounds the minimum opening of the valve needed in order to have a stable jet. When the valve position deviated from those thresholds, the jet would be instable.

It can be inferred that valve-opening values between 20 and 50 % would cause no problem when enough thickener was present in the mixture. In the case where no thickener is being added, the window of stability is expected to be way smaller. As the lowest thickener concentration studied was 0.75 g/l, it may only be assumed that slurries with extremely low viscosity, such as in the one with only water, would be more susceptible to jet-instability.

After, glasses were used to help observe the jet stability. Many effects are caused by a pulsating or vibrating jet, as can be seen in Figure 21, the glass milled with an unstable jet contains dotted lines, while a stable jet generate a result like showed in the picture on the right, it has continuous lines with variations imperceptible by eye.

It is also important to differentiate the two ways a jet can be instable. During the experiments, when the valve was too much opened, the instability would happen as a very low-frequency vibration that was visible as the hose moved. The other instability happened when the valve was closed beyond the threshold, avoiding enough slurry to flow proportionally to the vacuum created inside the mixing chamber. In this last behavior, bubbles of expanded air would be created in the hose carrying the slurry, and as air got to the mixing chamber, a pulsating jet would trow irregular amounts of abrasive as air and slurry came into it.

After the experiments with thickener, it was defined that a concentration of 2.5 g/l would be adopted to every slurry mixture done from now on. This value had good results in all experiments done until this step, for both abrasive settlement time and stability window. This value was also not expected to cause problems, such as with

Figure 20 – Jet stability based on the valve position.

Source: Own authorship.

Figure 21 – Glass test-pieces demonstrating the unstable (left) and stable (right) jets material-removing characteristics.

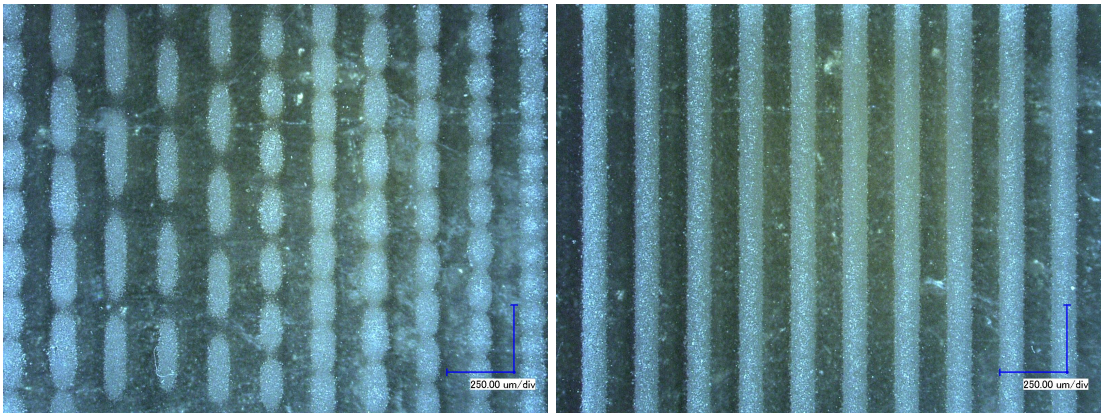

Source: Own authorship.

jet-shape or slurry flow-rate.

4.1.5 Milling Analysis with glass test-pieces

Before the final experiment with zirconia, glass pieces were milled in order to observe behaviors such as what would happen regarding the surface material removal. Nine pieces were processed directly with prepared batches of slurry, as they are pre-

sented in Figure 22. It is noticeable the different grove-size for each line made with the jet, depending on the input variables applied.

Figure 22 – Glass test-pieces used for removal rate investigations. Each one with its own identifier.

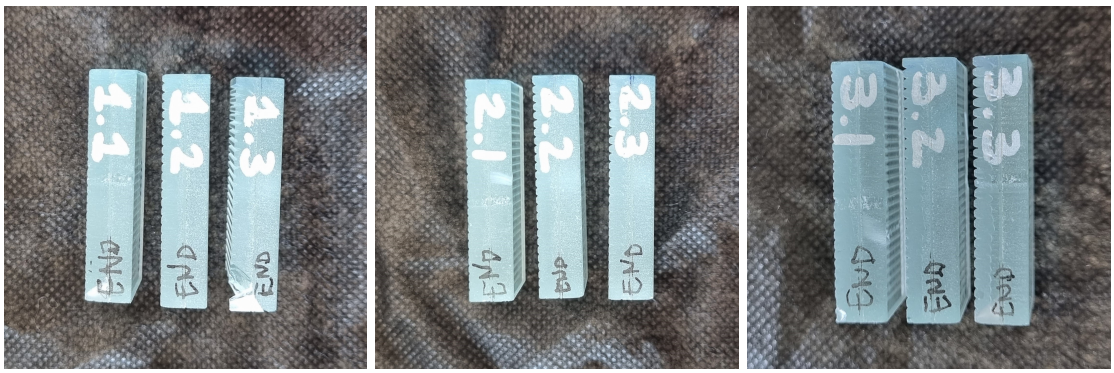

Source: Own authorship.

Results are first organized within Table 3. It is possible to observe the results directly on the images, just as the missing data in Glass 1.3 where the part was broken most likely by the forces involved in the process or by a problem with the preparation of the test-piece. Values of the average depth in each line are presented based on the input variables, increasing proportionally to the abrasive concentration and pressure, and decreasing when the traverse speed increases.

The data was processed with the use of the MATLAB script and then graphs generated from it. The analysis considered two main variables, the first being the Groves Depth Average, in Figure 23, and the second the Standard Deviation of the Groves Depth, in Figure 24.

It is important to reinforce that each variable combination was repeated five times (as five milled lines) in order to have a reliable result, the graphs used an average value based on each one. Values for 2000 bar with 1250 mm/min are unavailable, as the piece had this part broke and could not be measured, it is being shown as zero in the graphs.

The depth average is a good indicator for the material-removal capacity in each slurry mixture. As variables rise up, in slurry concentration and pressure, the groves' depth rise too. Other points that can be inferred with the depth average graphs are that with 2000 bar pressure, the depth value rises not in a specially constant and stable way, this can also be said when inspecting the values obtained with 1000 bar pressure. Values in the 1500 bar line have less variation in general. But a better analysis can be made next, together with the results from the Standard Deviation Depth.

As with Standard Deviation Depth, values showed to be low and stable in the lines with 1500 bar, specially when the milling was done with 5% abrasive concentration.

Table 3 – Experiment results achieved in with the nine glass test-pieces. When the value is not available, N.A. is showed instead.

Ident.	**Input Variables**		**Average Depth based on Traverse Speed (µm)**				
Exper. Number	**Abrasive Concentration (%)**	**Pressure (bar)**	**1250 mm/min**	**1000 mm/min**	**750 mm/min**	**500 mm/min**	**250 mm/min**
Glass 1.1	5	1000	255.57	189.62	373.37	123.29	103.47
Glass 1.2	5	1500	231.10	341.34	227.04	262.37	499.45
Glass 1.3	5	2000	N.A.	663.40	1529.68	1703.20	5159.65
Glass 2.1	7.5	1000	215.72	243.52	214.37	178.38	446.86
Glass 2.2	7.5	1500	339.27	350.78	262.96	569.52	1090.49
Glass 2.3	7.5	2000	311.99	593.24	1943.09	1937.35	2789.41
Glass 3.1	10	1000	168.51	183.72	121.94	151.13	591.88
Glass 3.2	10	1500	220.06	189.52	238.30	545.03	1367.98
Glass 3.3	10	2000	436.15	452.79	496.84	2211.75	6108.16

Source: Own authorship.

This pressure may not be considered the best one to generate stable results, when considering only the process done with 7.5%, but when done with 10%, values are also considerably good compared to the other pressures tested.

This experiment analysis was the last step to define many fixed variables used in the last experiment with Zirconia. The most promising results were obtained with a 1500 bar pressure, adopted for all the experiments from now on. The abrasive concentrations were chosen as values around 5% as this indicated to create a stable surface. Seven values for the abrasive concentration were chosen, 1%, 2.5%, 4%, 5%, 7.5%, 9%, and 10% as a way of finding the best results inside the selected window of investigation.

4.2 MULTI-STAGE PROCESSING WITH ZIRCONIA

Pre-roughed blocks were finished in processes with seven different slurry mixtures. The constitution of each mixture was defined based on all the previous experiments done. With the data gathered from Alicona, the software MountainsLab was then used to generate several reports for all the interesting data. The employment of such a software is justified by the need of a higher quality analysis that the scrip done in MATLAB was not able to do, but was not used before due to its limited use during the free-trial period. The report pattern put together is show in Figure 25 as an example of data studied with it.

Figure 23 – Depth average measured on the pieces of glass.

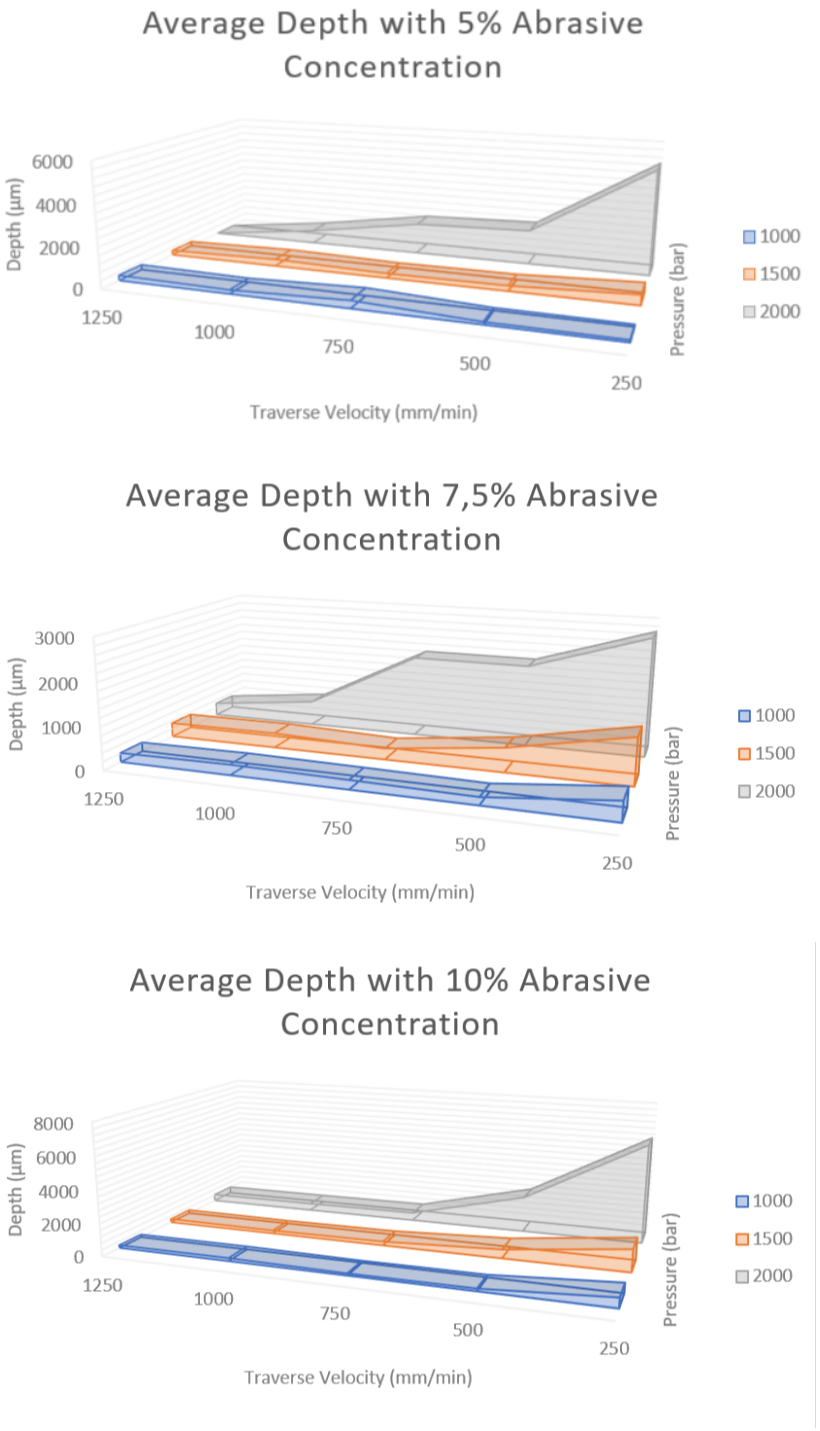

Source: Own authorship.

As the goal for these investigations has its focus on surface quality analysis, the report focused on mainly containing profile measurements, just as Surface Roughness and Waviness graphs in order to visually compare the trials. The surface roughness is an indicator to evaluate surface quality within a high-frequency filtered surface profile,

Figure 24 – Depth standard deviation measured on the pieces of glass.

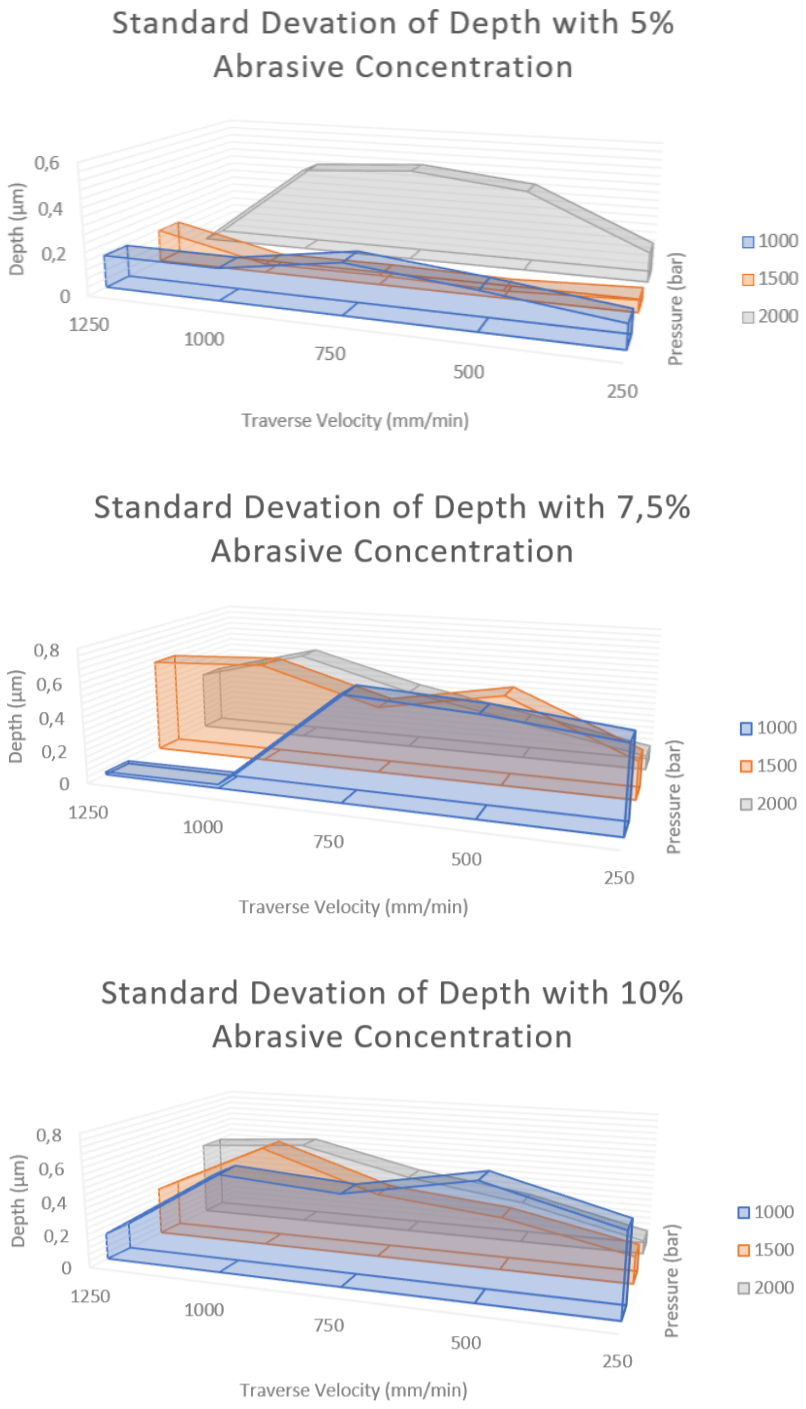

Source: Own authorship.

so high-frequency variations change this parameter more. The waviness is changed by low-frequency changes on the surface-profile, thus long changes in the material removal would change this value more. The report page was put together to show the following variables:

Figure 25 – Report built inside MountainsLab software.

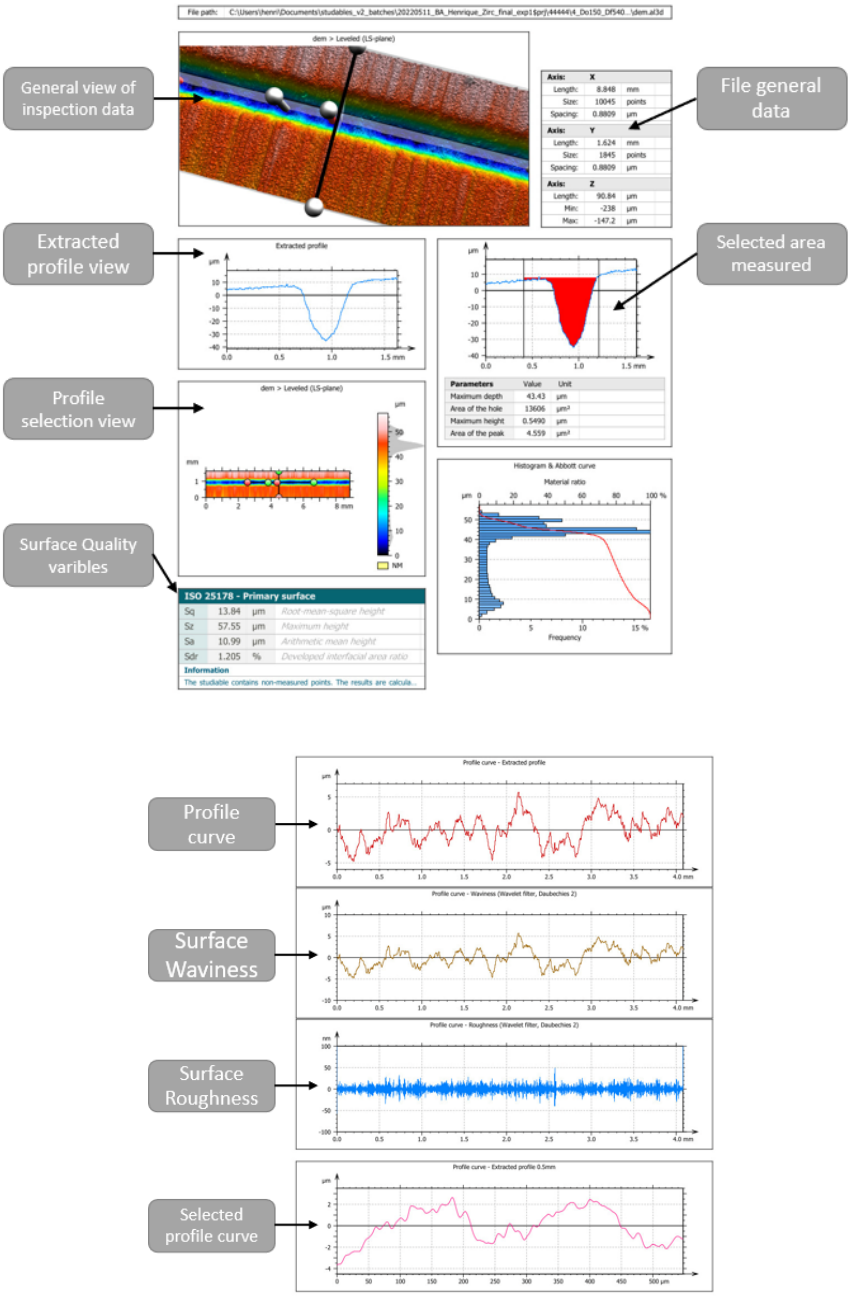

Source: Own authorship.

- General view of 3D data, together with the profile-lines selected.
- Parallel profile taken to allow view of depth and area.
- General analysis of surface quality with statistical analysis.
- Surface roughness analysis with graphs for Surface Roughness and Waviness.

Along with the PDF files, tables gathering all the data were generated for later analysis and creation of graphs, comparing the several experiment data gathered. Similar experiments, that had the same input variables, were grouped into a unique value as a mean of the values. A particularly important analysis can be made with the root-mean-square height data, in Figure 26.

The graphic was organized with a ranking of the test results from the best to the worst based on values of the average, maximum and minimum obtained from each group of trial results. The average value was the one taken to organize the order of them. Table 4 put the results together, with the bests highlighted for easier identification.

Trials with 5% abrasive concentration showed better results than the others for the variables of surface quality, so they are presented at the front part. Such results indicate that an approach with a bigger abrasive concentration and higher traverse speed create better values of Surface Waviness, but very high abrasive concentrations can deteriorate those values.

Results achieved with 7.5% and 10% abrasive concentration are also considerably good, just as with 5%, with 9% apparently being the threshold of abrasive concentration value. As for the low-concentration tests, the finishing process appears to have almost no effect, in the case with 2.5% concentration, the average method for ranking classified it as worse than the base roughed surface. Trials with 4% and 1% showed that lower quantities of abrasive do not cause enough material removal in order to improve surface quality.

When analyzing only the change that the traverse speed has into the root-mean-square value of the Height, it is observable that in the trials with good quantities of abrasive in the slurry, the higher traverse velocity would improve those values even further. With the experiments in which the abrasive concentration in the slurry were not sufficient, the traverse speed showed no big impacts, making an isolated analysis of such values might be inconclusive, that is why it was mainly discussed with the experiment with 5% abrasive concentration.

Table 4 – Root-mean-square results and comparison after finished milling process.

Identification	**Input Variables**	**Ranking of Root-mean-square Height values**		
Experiment Name	**Abrasive Concentration (%)**	**Average (µm)**	**Minimum (µm)**	**Maximum (µm)**
Roughed Zirconia	0	14.97	15.18	14.78
Finished Zirc 1%	1	14.89	15.36	14.81
Finished Zirc 2.5%	2.5	15.03	15.49	14.78
Finished Zirc 4%	4	14.70	14.88	14.58
Finished Zirc 5%	5	**13.34**	**13.69**	**13.13**
Finished Zirc 7.5%	7.5	13.59	**13.68**	13.35
Finished Zirc 9%	9	14.48	15.08	14.02
Finished Zirc 10%	10	13.76	14.02	13.36

Source: Own authorship.

Figure 26 – Comparative analysis between final results with Zirconia.

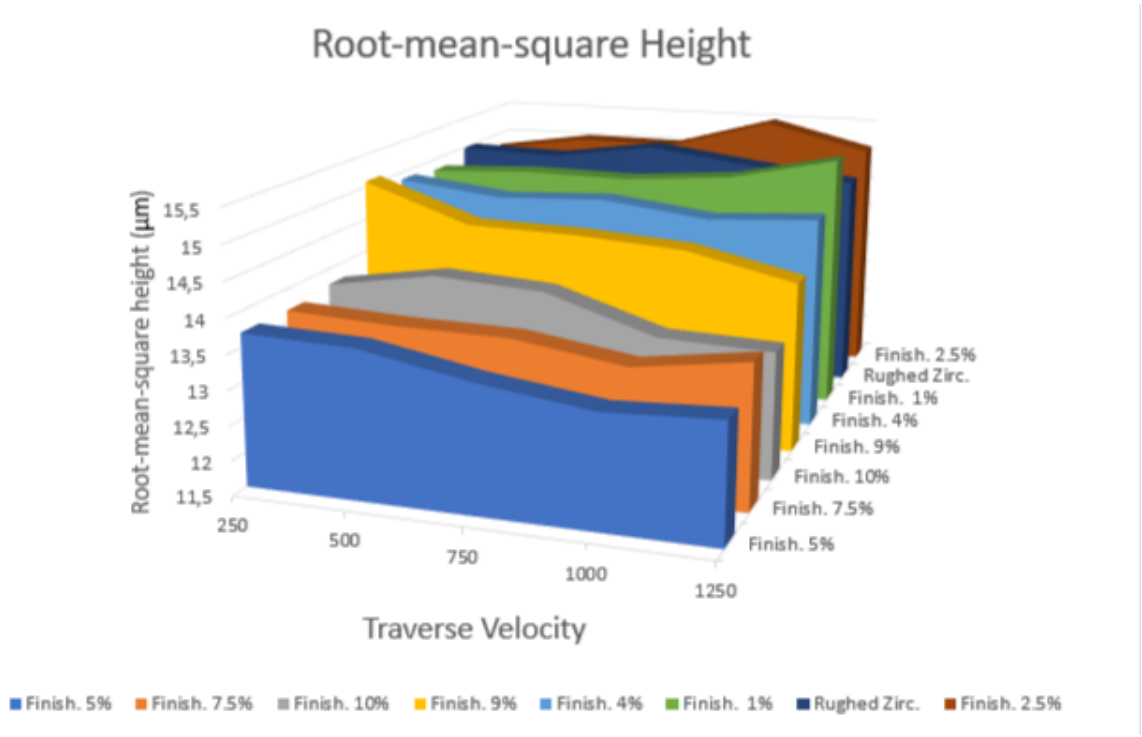

Source: Own authorship.

A deeper analysis can be made when comparing results from Surface Roughness and Waviness obtained from the two test-pieces. The roughed Zirconia, and the Zirconia with the finishing milling stage done with 1000 mm/min traverse velocity and slurry with 5% of abrasive concentration. Figure 27 show graphs of Surface Waviness and Roughness. Surface Waviness has less variation in the finished piece when compared to the roughed one, even though the Surface Roughness has apparently not changed drastically.

Although surface roughness appears to have not improved, results obtained with Surface Waviness enhance the improvement made in the processes. Even through not every experiment showed improvement in surface quality, such as with 2.5% concentration, they all showed improvements of some sort.

The final experiments served to narrow down values for the three most important input variables of the process: Pressure, traverse velocity, and abrasive concentration in the slurry. Even through many other possible combinations of those variables could be experimented with, values around a pressure of 1500 bar, a traverse speed of 1000 mm/min and an abrasive concentration of 5% are should give comparable results when repeating experiments such as the one done.

Figure 27 – Surface-quality analysis of roughed zirconia and selected finished surface. Graphs of surface waviness show an improvement in the finished zirconia (b) when compared to the roughed version (a). Surface roughness has only minor differences between them, indicating that no improvement was made.

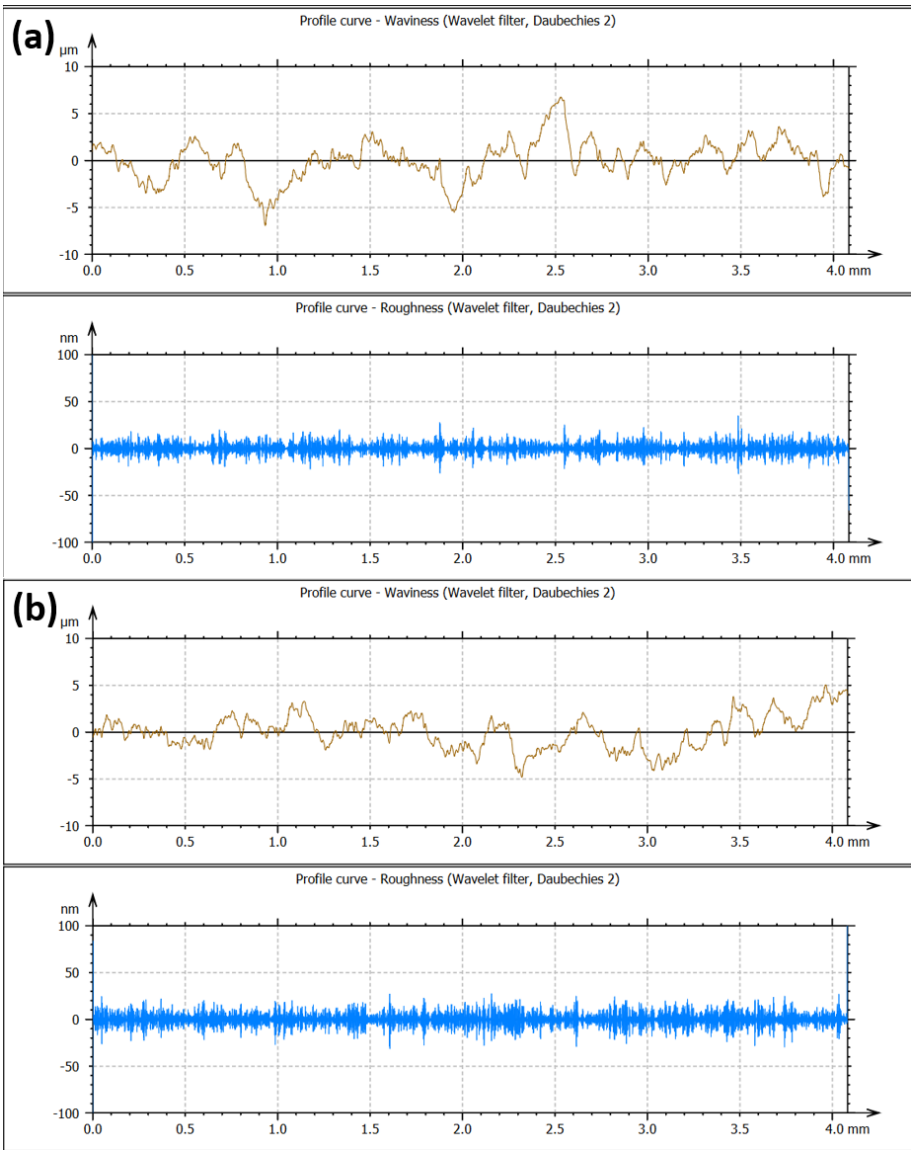

Source: Own authorship.

5 CONCLUSIONS AND FUTURE WORK

In this work, concepts related to Abrasive Water Jet (AWJ) and its variations were investigated. Initial experiments were done in order to achieve a stable jet in the process output, with use of a thickener added into the slurry. A brief comparison between the possibilities with each jet-type was made, and the use of Slurry Injection Abrasive Water Jet (iASJ) was adopted based on its characteristics. The application of multiple milling stages was considered to further improve results achieved with AWJ Milling, by a post-process with a special characterized jet tool: iASJ allows the use of finer grain-sized abrasives, but its industrial use still lacks in experience, enhancing the necessity of research done with iASJ.

Observations indicate that a stable jet is of great importance when controlling the amount of material removed per time, the MRR describe such amount. Pressure and traverse speed showed to have a linear influence in MRR, just as with the abrasive concentration of the slurry-mix. MRR would increase proportionally to pressure and abrasive concentration, and would decrease as traverse speed went up. Those results are comparable to what can be observed when milling with AWJ, even though the absence of air change the jet characteristics.

The iASJ process input-variables were successfully combined in a way to manually obtain a visually stable jet-flow. Jet-stability showed to be improved when a small quantity of thickener is added to the slurry. Experiments also characterized other effects on the general process: The addition of a thickener caused the abrasive to be maintained in suspension for longer. However, made no considerable changes in the jet-shape.

The use of iASJ Milling, together a multi-stage approach, generated better results than with the use of only AWJ and its traditional big-grained abrasive choices. Trials done with traverse velocity of 1000 mm/min and 5% Alumina abrasive concentration had better results in comparison to the trials with lower traverse speeds, and smaller abrasive concentrations. Comparison between pieces that were roughed and finished showed that Surface Waviness has improved in more than 10% while Surface Roughness showed no noticeable differences. In any case, the application of multi-stage reinforced the possibility to combine different approaches, such as AWJ for roughing of materials, and iASJ for finishing.

Future work can aim to create an automated system that supervise the jet-stability and automatically control the process input variables. It was difficult to manually change variables in order to achieve a stable jet when using slurry. Vibration analysis, or even visual inspections, can be made with aid of advanced control systems in order to evaluate the output and make corrections. Different abrasive types and grain-sizes can be considered in future investigations to further characterize their interaction with

the target material, together with the use of multiples milling stages. Another possibility is the use of a Ford Viscosity Cup, as to add new information about the slurry viscosity when adding thickeners to the mixture.

REFERENCES

ALICONA. **Alicona InfiniteFocus G4**. [S.l.]. Available from: https://www.alicona.com/en/products/infinitefocus. Visited on: 10 June 2023.

AXINTE, D. A.; KARPUSCHEWSKI, B.; KONG, M. C.; BEAUCAMP, A. T.; ANWAR, S.; MILLER, D.; PETZEL, M. High Energy Fluid Jet Machining (HEFJet-Mach): From scientific and technological advances to niche industrial applications. **CIRP Annals**, v. 63, n. 2, p. 751–771, 2014. ISSN 00078506. DOI: 10.1016/j.cirp.2014.05.001.

BERGS, T.; BORRMANN, J. P.; SCHÜLER, M.; HERRIG, T.; DÖRING, J.-E. Pure waterjet controlled depth machining for stripping ceramic thermal barrier coatings on turbine blades. **Procedia CIRP**, v. 85, p. 261–265, 2019. ISSN 22128271. DOI: 10.1016/j.procir.2019.09.029.

BERGS, T.; SCHÜLER, M.; DADGAR, M.; HERRIG, T.; KLINK, A. Investigation of Waterjet Phases on Material Removal Characteristics. **Procedia CIRP**, v. 95, p. 12–17, 2020. ISSN 22128271. DOI: 10.1016/j.procir.2020.02.319.

DADGAR, M.; SCHREINER, T.; SCHÜLER, M.; HERRIG, T.; BERGS, T. An Improved Model for Contour Damage Compensation in 3D Waterjet Machining. **Procedia CIRP**, v. 102, p. 387–392, 2021. ISSN 22128271. DOI: 10.1016/j.procir.2021.09.066.

DANTE, Roberto C. Abrasives, ceramic, and inorganic materials. In: HANDBOOK of Friction Materials and their Applications. [S.l.]: Elsevier, 2016. P. 105–121. ISBN 9780081006191. DOI: 10.1016/B978-0-08-100619-1.00008-0.

DESMORAT, RODRIGUE; LEMAITRE, JEAN. A Two-Scale Model for Quasi-Brittle and Fatigue Damage. In: HANDBOOK of Materials Behavior Models. [S.l.]: Elsevier, 2001. P. 525–535. ISBN 9780124433410. DOI: 10.1016/B978-012443341-0/50058-2.

EMELOGU, Adindu; MARUFUZZAMAN, Mohammad; THOMPSON, Scott M.; SHAMSAEI, Nima; BIAN, Linkan. Additive manufacturing of biomedical implants: A feasibility assessment via supply-chain cost analysis. **Additive Manufacturing**, v. 11, p. 97–113, 2016. ISSN 22148604. DOI: 10.1016/j.addma.2016.04.006.

GROTE, Karl-Heinrich; ANTONSSON, Erik K. **Springer Handbook of Mechanical Engineering**. Berlin, Heidelberg: Springer Berlin Heidelberg, 2009. ISBN 978-3-540-49131-6. DOI: 10.1007/978-3-540-30738-9.

HAGHBIN, Naser; AHMADZADEH, Farbod; SPELT, Jan K.; PAPINI, Marcello. High pressure abrasive slurry jet micro-machining using slurry entrainment. **The International Journal of Advanced Manufacturing Technology**, 2015. ISSN 0268-3768. DOI: 10.1007/s00170-015-7769-8.

K.G., Anbarasu; L., Vijayaraghavan; N., Arunachalam. Effect of multi stage abrasive slurry jet polishing on surface generation in glass. **Journal of Materials Processing Technology**, v. 267, p. 384–392, 2019. ISSN 09240136. DOI: 10.1016/j.jmatprotec.2019.01.001.

KLOCKE, F.; SCHREINER, T.; SCHÜLER, M.; ZEIS, M. Material Removal Simulation for Abrasive Water Jet Milling. **Procedia CIRP**, v. 68, p. 541–546, 2018. ISSN 22128271. DOI: 10.1016/j.procir.2017.12.110.

KOWSARI, K.; JAMES, D. F.; PAPINI, M.; SPELT, J. K. The effects of dilute polymer solution elasticity and viscosity on abrasive slurry jet micro-machining of glass. **Wear**, v. 309, n. 1-2, p. 112–119, 2014. ISSN 00431648. DOI: 10.1016/j.wear.2013.11.011.

KOWSARI, K.; SCHWARTZENTRUBER, J.; SPELT, J. K.; PAPINI, M. Erosive smoothing of abrasive slurry-jet micro-machined channels in glass, PMMA, and sintered ceramics: Experiments and roughness model. **Precision Engineering**, v. 49, p. 332–343, 2017. ISSN 01416359. DOI: 10.1016/j.precisioneng.2017.03.003.

MATHWORKS. **MATLAB**. [S.l.]. Available from: https://www.mathworks.com/products/matlab.html. Visited on: 10 June 2023.

MOMBER, Andreas W.; KOVACEVIC, Radovan. **Principles of Abrasive Water Jet Machining**. London: Springer London, 1998. ISBN 978-1-4471-1574-8. DOI: 10.1007/978-1-4471-1572-4.

NOURAEI, H.; KOWSARI, K.; PAPINI, M.; SPELT, J. K. Operating parameters to minimize feature size in abrasive slurry jet micro-machining. **Precision Engineering**, v. 44, p. 109–123, 2016. ISSN 01416359. DOI: 10.1016/j.precisioneng.2015.10.008.

OPENCV. **OpenCV**. [S.l.]. Available from: https://opencv.org/. Visited on: 10 June 2023.

PUTZ, M.; DIX, M.; MORCZINEK, F.; DITTRICH, M. Suspension Technology for Abrasive Waterjet (AWJ) Cutting of Ceramics. **Procedia CIRP**, v. 77, p. 367–370, 2018. ISSN 22128271. DOI: 10.1016/j.procir.2018.09.037.

RAMESH, Prabhu; MANI, Kanthababu. Prediction of surface roughness using machine learning approach for abrasive waterjet milling of alumina ceramic. **The International Journal of Advanced Manufacturing Technology**, v. 119, n. 1-2, p. 503–516, 2022. ISSN 0268-3768. DOI: 10.1007/s00170-021-08052-9.

RAMESHA, K.; SANTHOSH, N.; KIRAN, K.; MANJUNATH, N.; NARESH, H. Effect of the Process Parameters on Machining of GFRP Composites for Different Conditions of Abrasive Water Suspension Jet Machining. **Arabian Journal for Science and Engineering**, v. 44, n. 9, p. 7933–7943, 2019. ISSN 2193-567X. DOI: 10.1007/s13369-019-03973-w.

RIDDER, H.G. **H.G. Ridder Type WARICUT E-11045 Micro-max**. [S.l.]. Available from: https://www.waterjet-ridder.com/en_waricut_hwe.php. Visited on: 10 June 2023.

SANCHEZ, Irati; AXINTE, Dragos; SMITH, Rob. Modelling of rotational multiple plain water jets for controlled removal of multi-material coatings. **CIRP Annals**, v. 69, n. 1, p. 309–312, 2020. ISSN 00078506. DOI: 10.1016/j.cirp.2020.04.108.

SCHÜLER, M.; DADGAR, M.; HERRIG, T.; BERGS, T. Influence of Abrasive Properties on Erosion in Waterjet Machining. **Procedia CIRP**, v. 102, p. 375–380, 2021. ISSN 22128271. DOI: 10.1016/j.procir.2021.09.064.

SCHÜLER, M.; HERRIG, T.; BERGS, T. A study on abrasive waterjet multi-stage machining of ceramics. **Procedia CIRP**, v. 108, p. 770–775, 2022. ISSN 22128271. DOI: 10.1016/j.procir.2022.03.119.

SIEMENS. **Siemens SINUMERIK 840 - CNC Steuerungen**. [S.l.]. Available from: https://www.siemens.com/de/de/produkte/automatisierung/systeme/cnc-sinumerik/cnc-steuerungen/sinumerik-840.html. Visited on: 10 June 2023.

SRINIVASU, D. S.; AXINTE, D. An analytical model for top width of jet footprint in abrasive waterjet milling: a case study on SiC ceramics. **Proceedings of the Institution of Mechanical Engineers, Part B: Journal of Engineering Manufacture**, v. 225, n. 3, p. 319–335, 2011. ISSN 0954-4054. DOI: 10.1243/09544054JEM2101.

SURF, Digital. **MountainsLab**. [S.l.]. Available from: https://www.digitalsurf.com/software-solutions/multi-instrument/. Visited on: 10 June 2023.

TAZIBT, A.; PARSY, F.; ABRIAK, N. Theoretical analysis of the particle acceleration process in abrasive water jet cutting. **Computational Materials Science**, v. 5, n. 1-3, p. 243–254, 1996. ISSN 09270256. DOI: 10.1016/0927-0256(95)00075-5.

THYSSENKRUPP-UHDE. **ThyssenKrupp-Uhde HPS4022-OEM**. [S.l.]. Available from: https://www.thyssenkrupp-industrial-solutions.com/waterjet/en. Visited on: 10 June 2023.

ZENG, Jiyue; KIM, Thomas J. An erosion model for abrasive waterjet milling of polycrystalline ceramics. **Wear**, v. 199, n. 2, p. 275–282, 1996. ISSN 00431648. DOI: 10.1016/0043-1648(96)07223-7.

APPENDIX A – CNC CODE USED FOR EXPERIMENTS

```
G00 X0 Y0 Z0
G21 ;work with milim;
F1000
M3 ;turn on jet;
G01 X-5 Y1.25 ;INITIAL POINT;

F250 ;first 5 lines with this feedrate part 1;

G01 X25 Y1.25 ;line1;
G03 X25 Y2.75 I0 J0.75
G01 X-5 Y2.75 ;line2;
G02 X-5 Y4.25 I0 J0.75

G01 X25 Y4.25 ;line3;
G03 X25 Y5.75 I0 J0.75
G01 X-5 Y5.75 ;line4;
G02 X-5 Y7.25 I0 J0.75

G01 X25 Y7.25 ;line5;
G03 X25 Y8.75 I0 J0.75

F500 ;change of feedrate part 2;

G01 X-5 Y8.75 ;line6;
G02 X-5 Y10.25 I0 J0.75

G01 X25 Y10.25 ;line7;
G03 X25 Y11.75 I0 J0.75
G01 X-5 Y11.75 ;line8;
G02 X-5 Y13.25 I0 J0.75

G01 X25 Y13.25 ;line9;
G03 X25 Y14.75 I0 J0.75
G01 X-5 Y14.75 ;line10;
G02 X-5 Y16.25 I0 J0.75

F750 ;more 5 lines with this feedrate part 3;

G01 X25 Y16.25 ;line11;
G03 X25 Y17.75 I0 J0.75
```

```
41 G01 X-5 Y17.75 ;line12;
42 G02 X-5 Y19.25 I0 J0.75
43
44 G01 X25 Y19.25 ;line13;
45 G03 X25 Y20.75 I0 J0.75
46 G01 X-5 Y20.75 ;line14;
47 G02 X-5 Y22.25 I0 J0.75
48
49 G01 X25 Y22.25 ;line15;
50 G03 X25 Y23.75 I0 J0.75
51
52 F1000 ;change of feedrate part 4;
53
54 G01 X-5 Y23.75 ;line16;
55 G02 X-5 Y25.25 I0 J0.75
56
57 G01 X25 Y25.25 ;line17;
58 G03 X25 Y26.75 I0 J0.75
59 G01 X-5 Y26.75 ;line18;
60 G02 X-5 Y28.25 I0 J0.75
61
62 G01 X25 Y28.25 ;line19;
63 G03 X25 Y29.75 I0 J0.75
64 G01 X-5 Y29.75 ;line20;
65 G02 X-5 Y31.25 I0 J0.75
66
67 F1250 ;change of feedrate part 5;
68
69 G01 X25 Y31.25 ;line21;
70 G03 X25 Y32.75 I0 J0.75
71 G01 X-5 Y32.75 ;line22;
72 G02 X-5 Y34.25 I0 J0.75
73
74 G01 X25 Y34.25 ;line23;
75 G03 X25 Y35.75 I0 J0.75
76 G01 X-5 Y35.75 ;line24;
77 G02 X-5 Y37.25 I0 J0.75
78 G01 X25 Y37.25 ;line25;
79 G03 X25 Y38.75 I0 J0.75
80
81 M05 ;turn off jet;
```

APPENDIX B – COMPUTER-VISION JET-SHAPE ANALYSIS CODE

```
import cv2
import numpy as np
import matplotlib.pyplot as plt
import os
import pandas as pd

# Directory containing the PNG files
directory = "jatos_para_analizar/"

# List to store the measured data
data = []

# Process each PNG file in the directory
for filename in os.listdir(directory):
    if filename.endswith(".JPG"):
        # Load the image
        image = cv2.imread(os.path.join(directory, filename))

        # Convert the image to grayscale
        gray = cv2.cvtColor(image, cv2.COLOR_BGR2GRAY)

        # Perform image segmentation
        _, threshold = cv2.threshold(gray, 127, 255, cv2.
            THRESH_BINARY)

        # Find contours in the segmented image
        contours, _ = cv2.findContours(threshold, cv2.RETR_EXTERNAL
            , cv2.CHAIN_APPROX_SIMPLE)

        # Select the segmented image containing the center point
        center = (image.shape[1] // 2, image.shape[0] // 2)
        selected_contour = None
        for contour in contours:
            if cv2.pointPolygonTest(contour, center, False) >= 0:
                selected_contour = contour
                break

        # Create a blank image to draw the contours and lines
        output = np.zeros_like(image)

```

```
39          # Draw green contour around the segmented image
40          cv2.drawContours(output, [selected_contour], -1, (0, 255,
                0), 50)
41
42          # Calculate the centroid of the selected contour
43          M = cv2.moments(selected_contour)
44          centroid_x = int(M['m10'] / M['m00'])
45          centroid_y = int(M['m01'] / M['m00'])
46          centroid = (centroid_x, centroid_y)
47
48          # Draw a purple dot at the centroid
49          cv2.circle(output, centroid, 10, (255, 0, 255), 20)
50
51          # Draw a red vertical line through the center of the
                segmented image
52          cv2.line(output, (center[0], 0), (center[0], image.shape
                [0]), (0, 0, 255), 20)
53
54          # Calculate the starting and ending points for the blue
                line
55          start_point = (centroid_x, centroid_y - 500)
56          end_point = (centroid_x, centroid_y + 500)
57
58          # Draw a blue line as the average line
59          cv2.line(output, start_point, end_point, (255, 0, 0), 30)
60
61          # Calculate the angle between the blue line and the red
                line
62          angle = np.arctan2(end_point[1] - start_point[1], end_point
                [0] - start_point[0]) - np.arctan2(center[1] -
                centroid_y, center[0] - centroid_x)
63          angle = np.degrees(angle)
64          if angle < 0:
65              angle += 360
66
67          # Calculate the width measurements
68          width_measurements = []
69          y_positions = []
70          for i in range(5):
71              y_position = centroid_y + 500 - (i * 500)
72              y_positions.append(y_position)
73              width = np.sum(threshold[y_position, :]) // 255
```

```
74              width_measurements.append(width)
75
76          # Append the measured data to the list
77          data.append([filename] + list(zip(y_positions,
                width_measurements)) + [angle])
78
79          # Save the image with overlaid data
80          output_with_data = output.copy()
81          for i, (y, width) in enumerate(zip(y_positions,
                width_measurements)):
82              cv2.putText(output_with_data, f"y: {y}", (20, y), cv2.
                    FONT_HERSHEY_SIMPLEX, 1, (255, 255, 255), 2)
83              cv2.putText(output_with_data, f"Width {i+1}: {width}px"
                    , (50, y + 30), cv2.FONT_HERSHEY_SIMPLEX, 1, (255,
                    255, 255), 2)
84          cv2.putText(output_with_data, f"Angle: {angle:.2f} degrees"
                , (50, 50), cv2.FONT_HERSHEY_SIMPLEX, 1, (255, 255, 255)
                , 2)
85
86          # Overlay the data on the original image
87          output_with_image = cv2.addWeighted(output_with_data, 0.7,
                image, 0.3, 0)
88
89          # Save the overlaid image
90          cv2.imwrite(os.path.join(directory, f"{filename}_with_data.
                jpg"), output_with_image)
91
92  # Create a DataFrame from the measured data
93  columns = ["Image"] + [f"Y{i+1}" for i in range(5)] + [f"Width{i+1}
        " for i in range(5)] + ["Angle"]
94  df = pd.DataFrame(data, columns=columns)
95
96  # Save the DataFrame as an Excel file
97  df.to_excel("measured_data.xlsx", index=False)
```